Physical Chemistry Chemical Physics

PCCP

Experiment and theory confirm that UV laser photodissociation spectroscopy can distinguish protomers formed via electrospray

Journal:	*Physical Chemistry Chemical Physics*
Manuscript ID	CP-ART-04-2017-002817.R1
Article Type:	Paper
Date Submitted by the Author:	n/a
Complete List of Authors:	Matthews, Edward; University of York, Department of Chemistry Dessent, Caroline Elizabeth Helen; University of York, Department of Chemistry

Article type: Full paper

Website www.rsc.org/pccp
Impact factor* 4.449

Journal expectations To be suitable for publication in *Physical Chemistry Chemical Physics* (*PCCP*) articles must include significant new insight into physical chemistry.

Article type: Full paper Original scientific work that has not been published previously. Full papers do not have a page limit and should be appropriate in length for scientific content.

Journal scope Visit the *PCCP* website for additional details of the journal scope and expectations.

PCCP is an international journal for the publication of cutting-edge original work in physical chemistry, chemical physics and biophysical chemistry. To be suitable for publication in *PCCP*, articles must include significant new insight into physical chemistry; this is the most important criterion that reviewers should judge against when evaluating submissions. Example topics within the journal's broad scope include:

- Spectroscopy
- Dynamics
- Kinetics
- Statistical mechanics
- Thermodynamics
- Electrochemistry
- Catalysis
- Surface science
- Quantum mechanics
- Theoretical research

Interdisciplinary research areas such as polymers and soft matter, materials, nanoscience, surfaces/interfaces, and biophysical chemistry are also welcomed if they demonstrate significant new insight into physical chemistry.

Reviewer responsibilities Visit the Reviewer responsibilities website for additional details of the reviewing policy and procedure for Royal of Society of Chemistry journals.

When preparing your report, please:

- Focus on the originality, importance, impact and reliability of the science. English language and grammatical errors do not need to be discussed in detail, except where it impedes scientific understanding.
- Use the journal scope and expectations to assess the manuscript's suitability for publication in *PCCP.*
- State clearly whether you think the article should be accepted or rejected and include details of how the science presented in the article corresponds to publication criteria.
- Inform the Editor if there is a conflict of interest, a significant part of the work you cannot review with confidence or if parts of the work have previously been published.

Thank you for evaluating this manuscript, your advice as a reviewer for *PCCP* is greatly appreciated.

Dr Anna Simpson Executive Editor
Royal Society of Chemistry, UK

Professor Seong Keun Kim Editorial Board Chair
Seoul National University, South Korea

**2015 Journal Citation Reports®, (Thomson Reuters, 2016)*

THE UNIVERSITY of York

DEPARTMENT OF CHEMISTRY
University of York
Heslington, York YO10 5DD
Enquiries:+ 44 (0)1904 432511
Facsimile: + 44 (0) 1904 432516

Dr C E H Dessent
Direct Telephone + 44 (0)1904 324092
E-mail: caroline.dessent@york.ac.uk

14 June 2017

Associate Editor, *Physical Chemistry Chemical Physics*

Dear Professor Albinsson,

We enclose a revised electronic version of the manuscript CP-ART-04-2017-002817,

Experiment and theory confirm that UV laser photodissociation spectroscopy can distinguish protomers formed via electrospray,

Edward Matthews and Caroline E. H. Dessent

We have revised the manuscript to take account of all of the comments of the referees. Our responses to the referee's comments, along with a description of changes made to the manuscript, are included in the enclosed response to referees document.

We hope the manuscript will now meet with your approval and look forward to hearing from you in due course.

Yours sincerely,

Caroline Dessent

Response to Referees: CP-ART-04-2017-002817

Referee 1

We were pleased that this referee found the manuscript to bevery interesting, and the conclusions well-supported by the data. In reply to the referee's comments about the data analysis:

1. and 2. In our original data analysis, we corrected the spectra for laser power by following a method given in Ref 11 of the manuscript. However, having considered this in light of the referee's comments, we agree that this method is not the most generally used, and have therefore reverted to the "standard" correction of dividing by power x wavelength that is used widely in this field. (See for example, Compagnon et al, PCCP, 12, 3399, 2010, and also references 21, and 26 of the manuscript). The laser power employed in the study was in line with our standard practice, but the saturated peak, corresponds to a very strong transition. We were not aware of this until after the experimental run. The laser power used in the experiment was chosen to optimize the overall spectra, and in particular to give good signals for the weaker bands. We are confident that this issue in no way affects the overall interpretation of our data. To illustrate that essentially the same qualitative spectra are obtained irrespective of power correction, we have copied the two versions (old – used in original manuscript) and new (used in the revised manuscript) in the appendix at the end of this response.

3. The deconvolution of the photofragment spectra into Gaussians, was done to allow a better quantitative value to be obtained for the electronic excitation energies (included in Table 2). It is very clear from the appearance of the bands in the photofragment spectra that the observed bands display partially resolved structure. On balance, our fitting of the Gaussians was not clearly described in the original version of the manuscript. To correct this, we have moved the deconvolution of the photofragments into the ESI (new section S5 of the ESI). The Gaussian fits have been entirely removed from Figure 4 of the manuscript, and the text adjusted to take account of the modifications to the figure.

4. We are certainly aware of the application of UV action spectroscopy to protonated nucleobases, where tautomers have been identified. We had chosen to omit direct reference to these works as in the original study by Weinkauf and co-workers, the action spectra were not measured in mass-resolved photofragment channels, allowing individual isomers to be clearly identified, as in our current work. However, we agree that this study may be of interest to readers, and have therefore included a reference with a suitable sentence in footnote 19 (New Reference 23). We also added reference to the dynamical study of protonated adenine conducted at the same time by Nielsen and co-workers for completeness. The very recent work of Jouvet and co-workers is distinctive from our work as it has been conducted at much higher resolution in a cryogenically cooled set up. However, we again include a sentence and reference linking to this in footnote 19 so that this area is fully covered.

Referee 2

In response to the opening comments of this referee, we direct the reader to our remarks in response to a similar comment from Referee 3 (point 3). To address the specific comments of this referee:

1. p7, l.5: We agree with the referee's suggestion and have amended the sentence so that it now says: "..the peak of band I appears truncated in the spectrum…"

2. p8, l.21: We agree that the language suggested by the referee is clearer than our previous phrasing and have therefore amended the sentence so that it now reads as follows "the overlap between bands II and III means that both the **PABA-OH$^+$** and **PABA-NH$_3^+$** isomers are present and cannot be resolved."

3. p18, l1: There seems to be some confusion here. It seems that the referee has understood that we are saying that exactly the same protomeric species is being transferred from solution to the gas-phase. (His objections would be fully warranted if this was the case.) Our point is simply that the appearance of the UV spectrum of a particular isomer in the gas-phase resembles the UV spectrum of that same isomer when it is present in solution. By assigning a particular gas-phase spectrum to a particular isomer, we are therefore able to understand which protomer is present in the bulk solution. To make this clearer at the point in the text that the referee has noted, we have added the following sentence: (i.e. the UV spectrum of a given protomer is essentially the same in the gas-phase and in the solution-phase, thus allowing us to identify a species that is present in solution once the same isomer has been identified in the gas-phase.)

4. p.18, l.13: We have amended our comments on the situation with IRMPD to take account of the referee's comment. The text now reads:

"xxx"

We have also removed all the = signs after m/z throughout the manuscript to meet the referee's request, and also changed dm^3 to L.

5. SI p.4: The referee has noticed an error in the text of the SI. The sentence in question was left behind when we removed some additional discussion relating to photofragments. We have deleted the phrase below from the revised ESI:

"The photofragment production spectra that are given in section S4 suggest that m/z = 120 and 94 may be responsible for the difference."

6. SI p.17: Again, there seems to be some possible confusion here. We were not implying that PABA is already protonated in neutral solution conditions (it is only protonated below pH=2.4, see Van de Graaf, et al, J. Org. Chem, 1981, 46, 653.) but simply that none of the OH protonated form is present in solution. To make this clear, we have amended the SI text at this point by adding the phrase:

"(i.e. even under these conditions, there is no **PABA-OH$^+$** present)."

Referee 3

We were pleased that this referee agreed that our paper constituted a well-done piece of work. The referee makes two further points:

1. Lowering the HF component of B3LYP below 5%: We agree with the referee that lowering the HF component of B3LYP might have led to better agreement with the experimental spectrum. However, such corrections are always open to some discussion as to their generality, and in our current work, we were concerned to present calculations at the highest possible practicable level, where, and therefore chose to conduct the high-level SORCI/MRCI calculations presented in the main text.

2. To address the referee's comment the UV action has recently been used to identify electrosprayed isomers, we have added a sentence to footnote 19, stating "We note that other isomers have also been spectroscopically identified by UV photodissociation. Ref [26] provides a recent example where UV action spectroscopy has been used to identify peptide isomers generated via electron transfer dissociation."

3. The referee then comments that "the main problem with publishing this work is the same as the editorial comment from the previous submission". Our response to this is that it is important to note that the previous submission was to *Chemical Science*, where the editors are focused on rejecting a substantial percentage of submissions. We believe that it is unfair to judge the current manuscript in light of an editor's decision which is specifically for its suitability in *Chemical Science*. Moreover, this referee seems to contradict himself when he states that the paper (which we note represents a very substantial body of experimental and theoretical work) should be published as supporting information to accompany another, new study. This comment indicates to us that the referee believes that the material in the paper would be an essential building block towards more widely applying this technique, and (as we have argued in our original submission letter) therefore we stand strongly behind the importance of the work presented in this paper, and its suitability for publication in PCCP.

We reject the referee's comment that we should not have chosen to study p-aminobenzoic acid because much is known about it. Surely, only by demonstrating the applicability of our technique on a prototype system can we confidently go on to use it on new, chemical and biochemical systems. Without the definitive demonstration that we present in this paper, any future studies we submit for publication would be open to criticism that our approach had not been properly validated, given the ambiguities that we met in previous submission (our JPC A article on nicotinamide). Finally, we would also note that PCCP has very recently published another article on characterisation of the protonated PABA system. (J. Seo, S. Warnke, S. Gewinner, W. Schollkopf, M. T. Bowers, K. Pagel and G. von Helden, *Phys. Chem. Chem. Phys.*, 2016, **18**, 25474-25482.) We believe that the technique demonstrated by us in the current paper is considerably more novel than the IMS/IR techniques used in this recent PCCP article. Presumably, the PCCP editors decided on that occasion that the manuscript was worth publishing given the very central role that p-aminobenzoic acid plays as a prototype system. We believe that our manuscript merits publication under the same considerations applied to the manuscript of Seo et al.

Appendix (See response to Referee 1)

Figure 2 presented with old and new power corrections

(Old) Power raised to 0.492

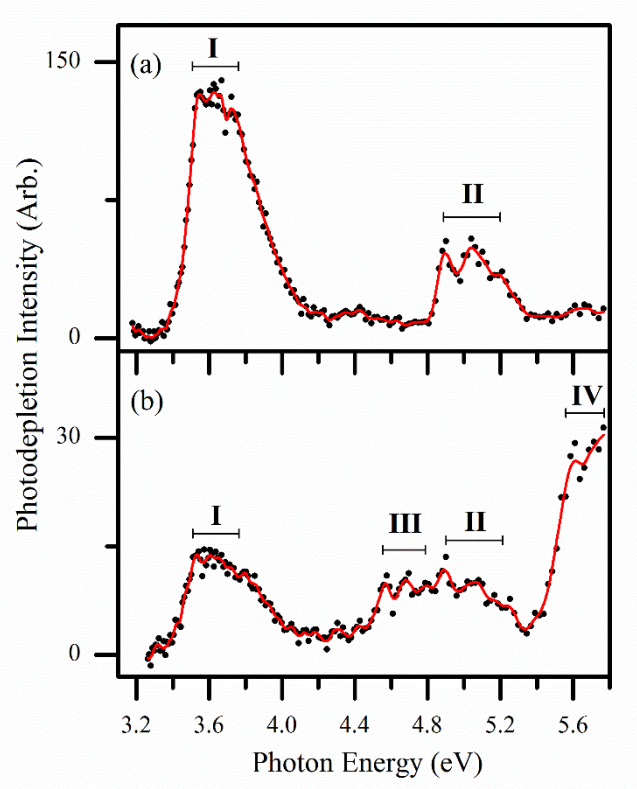

(New) $\ln(I_{off}/I_{on})$/power x wavelength (standard correction)

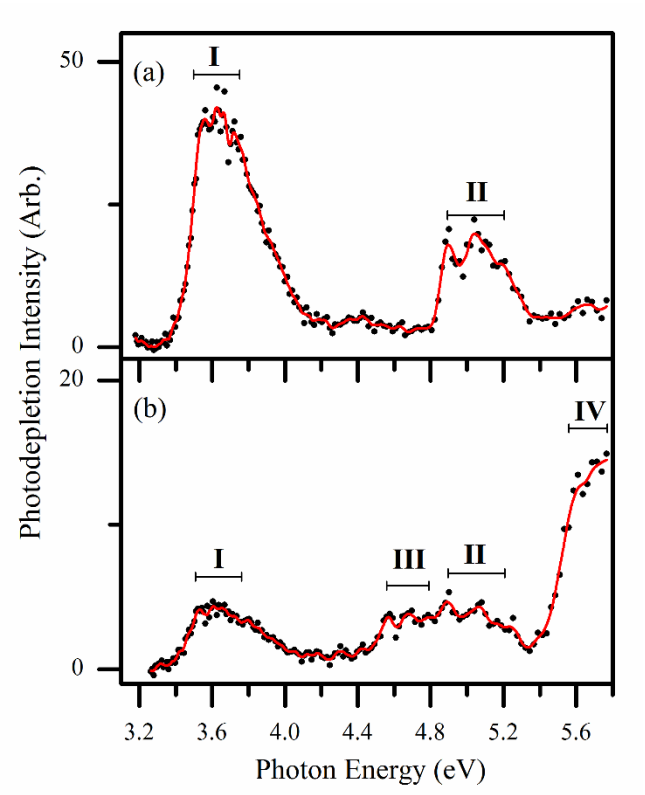

Experiment and theory confirm that UV laser photodissociation spectroscopy can distinguish protomers formed via electrospray

Edward Matthews and Caroline E. H. Dessent*

Department of Chemistry, University of York, Heslington, York, YO10 5DD, UK.

Abstract

The identification of protonation sites in electrosprayed molecules remains a challenge in contemporary physical science. We present the first demonstration that low-resolution, UV laser photodissociation spectroscopy can be applied *in situ* to identify the protomers of *para*-aminobenzoic acid (PABA) formed via electrospray from a single solution. Electronic absorption spectra are recorded via photodepletion and photofragmentation for PABA electrosprayed from solutions of water and acetonitrile. Using this approach, two protomers can be straightforwardly identified, with only the carboxylic acid protomer being produced on electrospray from water while the amine-protonated isomer dominates upon electrospray from acetonitrile. High-level SORCI and MRCI calculations are presented to provide insight into the origin of the distinctive electronic spectra displayed by the protomers. Our results are in excellent agreement with previous PABA studies conducted using established techniques, and demonstrate that UV photodissociation spectroscopy of electrosprayed ions has potential as a new diagnostic tool for identifying protomeric species.

* Corresponding Author: caroline.dessent@york.ac.uk

Introduction

The influence of electrospray ionisation on the structure and properties of gaseous ions has been the subject of much debate in recent years, particularly in relation to the influence of electrospray on the location of protonation and deprotonation sites in the ions formed.[1-14] These studies are driven by the importance of acid-base reactions throughout chemistry and biology, so that correctly identifying the structures of protonation and deprotonation isomers can be crucial to understanding reactive processes. Electrospray ionization has been successfully employed across analytical chemistry for many years, and is now being increasingly used to probe solution-phase reactions and reactive intermediates for both chemical and biochemical systems.[15-18] The influence of the electrospray process on the location of protonation and deprotonation sites is therefore of ongoing key chemical interest. Moreover, it is of critical importance to develop innovative experimental methods that can determine the structures of gaseous protomers *in situ* following electrospray ionisation.

Protomer formation in small organic molecules following electrospray has been investigated by a number of mass-spectrometry methods. The effect of varying the electrospray source conditions (e.g. the solvent used in electrospray) on protomeric ratios was explicitly investigated in a number of these studies.[4,6] The first such studies employed collision induced dissociation as a structural tool,[1-3] and both ion mobility mass spectrometry (IMMS),[4-10] and infrared multiphoton dissociation (IRMPD) were subsequently employed.[9-13] These studies have led to an emerging view that the electrospray conditions can strongly influence the ratios of protomers or deprotomers obtained following electrospray.[11,12] This conclusion is in distinct contrast with the more traditional view that molecular ion populations obtained via

electrospray reflect the solution-phase populations.[4,11,12] Ultimately, this situation means that it is essential to have effective methodologies available that can experimentally identify protomeric species formed in the gas-phase via electrospray.

In a recent study, we investigated the electronic spectroscopy of the protonated form of the vitamin nicotinamide, generated via electrospray. [14] Our UV photodissociation (UVPD) results were consistent with two different protomers of nicotinamide being formed upon electrospray. This result suggested that UVPD spectroscopy could have potential as a new diagnostic spectroscopic tool for identifying protomeric isomers formed from a single solution.[19-22] UVPD spectroscopy offers considerable potential as a technique for identifying different protomers as resonant UV absorption is likely to be highly sensitive to the electronic structure of the chromophore.

In this work, we aim to evaluate UVPD for identifying electrosprayed protomers by investigating the prototype molecule, *para*-aminobenzoic acid (PABA). PABA has been extensively studied in both the solution phase and gas phases as a paradigm molecule which possesses two protonation sites (Fig. 1), namely the carboxylic oxygen (**PABA-OH$^+$**) and the amine nitrogen, (**PABA-NH$_3^+$**). While the **PABA-OH$^+$** protomer is the most stable protomer in the gas-phase, this situation is reversed in the solution phase where **PABA-NH$_3^+$** is most stable. [2, 10, 11, 13, 27, 28]

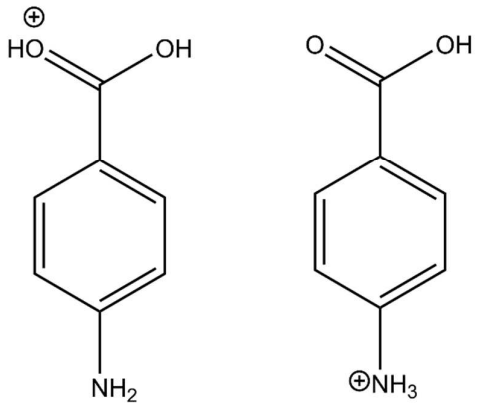

Fig. 1 Schematic diagram of the **PABA-OH**$^+$ and **PABA-NH$_3$**$^+$ protomers of PABA·H$^+$, illustrating the lowest energy protonation sites.

From the previous studies of electrosprayed PABA, it has been established that the gaseous protomers produced depend strongly on the electrospray solvent. Kass and co-workers found that **PABA-OH**$^+$ was the only gaseous structure when a water/methanol solvent mixture was employed, while both the **PABA-NH$_3$**$^+$ and **PABA-OH**$^+$ protomers were observed when a water/acetonitrile solution was used.[2, 11] These results were subsequently confirmed in an IMMS and IRMPD study.[10] Williams and co-workers were able to demonstrate that the structure of microhydrated PABA·H$^+$ moves from the **PABA-OH**$^+$ isomer to the **PABA-NH$_3$**$^+$ structure as the number of solvating water molecules increases.[13] Therefore, in this study, the UVPD spectra of protonated PABA produced from solutions of both water and acetonitrile will be measured, with the expectation that this change in solvent should produce dramatically different gaseous populations of the two possible protomers. This should allow us to firmly establish whether UVPD is able to distinguish such protomeric species, generated from a single solution. High-level SORCI and MRCI calculations are also performed to

allow us to confirm the spectroscopic assignments, as well as to provide a basis for understanding any differences in the electronic spectroscopy of different protomers.

Methodology

Experimental

The gaseous ion absorption spectra was recorded *in vacuo* using action spectroscopy. UV photodissociation experiments were conducted in an AmaZon ion-trap mass spectrometer, which was modified for the laser experiments as described in detail elsewhere.[14, 29] UV photons were produced by an Nd:YAG (10 Hz, Surelite) pumped OPO (Horizon) laser, giving ~1 mJ across the range 380 - 215 nm (3.26 – 5.77 eV). Scans were conducted using a 1 nm step size. Photofragmentation experiments were run with an ion accumulation time between 20 – 100 ms with a fragmentation time of 100 ms, ensuring an average of one laser pulse per ion packet. Total absorption is taken as the depletion in ion intensity of mass-selected PABA·H^+ ions, following irradiation, according to Equation [1]:

$$\text{Photodepletion Intensity} = \text{Ln}\left(\frac{\text{Int}_{OFF}}{\text{Int}_{ON}}\right)/P\lambda \qquad [1]$$

Where Int_{ON} and Int_{OFF} are the intensities of the PABA·H^+ ion signal with and without irradiation respectively, P is the tuneable laser power (mJ), and λ the wavelength (nm), following Ref [14]. (Section S1 of the ESI† presents power dependence measurements conducted as part of this work). The photodepletion intensities of mass selected PABA·H^+ ions have been averaged at each wavelength across the range 380 - 215 nm are plotted against the energy of the excitation photons. The production of photofragments that are associated with the depletion of PABA·H^+ ions is calculated using Equation [2], where Int_{Frag} is the ion intensity of an individual photofragment at a particular wavelength.

$$\text{Photofragmentation Production} = \left(\frac{\text{Int}_{Frag}}{\text{Int}_{OFF}}\right) / P\lambda \qquad [2]$$

Solutions of PABA (1 x 10^{-4} mol L^{-1}) in deionised water or acidified acetonitrile (32 μL acetic acid in 100 mL of MeCN) were introduced to the mass spectrometer through electrospray ionisation (ESI) using a nebulising gas pressure of 10.0 psi, an injection rate of 300 μL/hr, a drying gas flow rate of 8.0 L min^{-1}, and capillary temperatures of 140 and 200°C for water and MeCN respectively. A small volume of acetic acid was added to the MeCN solvent, since this was found to significantly improve the intensity and stability of the electrosprayed PABA·H^+ ion signal. Increasing the capillary temperature for MeCN also improved the stability of the ion signal. PABA was purchased from Fisher Scientific Ltd and used without purification. The voltages applied to the ion optics were tuned to maximise the ion signal of PABA·H^+ (m/z 138) using the automated tuning capabilities of the trapControl (Bruker) software.

Computational

Structures of PABA·H^+, protonated at each carbon, nitrogen and oxygen atom, were optimised using the B3LYP/6-311+G(2d,2p) functional and basis set using Gaussian 09.[30-35] Frequency calculations were performed to ensure that all optimised structures correspond to true energy minima. Time-dependent density functional theory (TDDFT) calculations were performed on the optimised structures of **PABA-NH_3^+** and **PABA-OH^+**, at the B3LYP/6-311+G(2d,2p) level. The B3LYP optimised structures of **PABA-NH_3^+** and **PABA-OH^+** were re-optimised at the MP2/6-311+G(2d,2p) level,[36] and these optimised structures were used as starting points in excited state calculations using the quantum chemical package ORCA.[37] Vertical excitation energies were calculated using the SORCI and MRCI methods,[38] with full details of the calculations given in Section S2 of the ESI†. These calculations used a CASSCF(6,6) reference space. Details of the generation and selection of orbitals are also

given in the ESI†. All excited state calculations using ORCA were performed using the aug-cc-pVDZ basis set.[39]

Results and Discussion

Photodepletion absorption spectra of PABA·H$^+$

The UV absorption spectrum of mass-selected PABA·H$^+$, electrosprayed from water, is shown in Fig. 2a. This spectrum has an absorption onset at 3.3 eV and contains two well-resolved features; a strong band (**I**), observed between 3.4-4.1 eV (peaks between 3.6-3.8 eV), and a weaker band (**II**) that appears between 4.8-5.4 eV. We note that the "peak" of band **I** appears truncated in the spectrum shown in Fig. 2a. Power studies conducted at 3.63 eV (Section S1 of the ESI†), show that photodepletion is effectively flat for laser pulse energies > 0.6 mJ, indicating that all PABA·H$^+$ ions that spatially overlap with the laser are fragmenting at this excitation energy. Under the experimental conditions (laser pulse energy ~ 1 mJ), the water-electrosprayed photodepletion spectrum is therefore saturated between

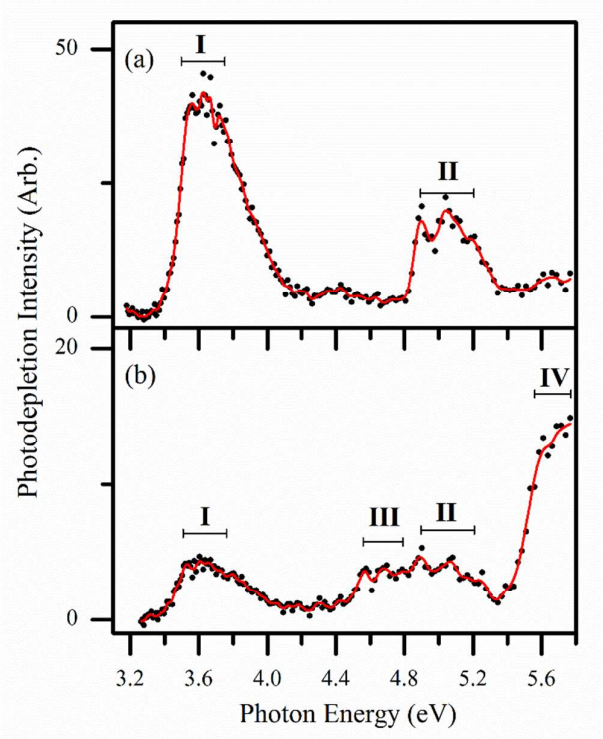

Fig. 2 UV absorption spectra of electrosprayed PABA·H$^+$ ions (m/z 138) across the range 3.26-5.77 eV (380-215 nm), produced from solutions of a) water and b) acidified-MeCN. The solid red lines are three-point adjacent averages of the data points.

3.55-3.75 eV.

Fig. 2b displays the corresponding UV absorption spectrum of PABA·H^+ formed from electrospray of a solution of acidified MeCN. The difference between this spectrum and the spectrum obtained from water is dramatic. The Fig. 2b spectrum contains the bands **I** and **II** that were observed in the spectrum of PABA·H^+ electrosprayed from water, along with two additional bands; a weak band between 4.5-4.8 eV (**III**) that overlaps with band **II**; and a strong band observed above 5.4 eV which peaks above 5.8 eV (**IV**). We note that fine structure can be seen in bands **II** and **III** of Fig. 2, and this is attributed to vibronic coupling which has been observed in the gaseous electronic absorption spectrum of neutral PABA.[40, 41] The observation of four absorption bands in the spectrum obtained from the MeCN solution, including the previously observed bands **I** and **II**, indicates that there are at least two distinctive species present in the gas phase when the PABA·H^+ ion is electrosprayed from MeCN. Since the irradiated ions have been mass-selected, the new species can be unambiguously assigned as a different structural isomer of PABA·H^+. The observation of one PABA·H^+ protomer when the electospray solvent is protic and two PABA·H^+ protomers when the solvent is aprotic is entirely expected from the previous studies reviewed in the introduction.[2, 11] Based on these previous studies, we therefore attribute the UV absorption spectrum obtained by electrospraying from an aqueous solution (Fig. 2a) as corresponding solely to the **PABA-OH**$^+$ protomer, while the spectrum obtained by electrospraying from acetonitrile corresponds to a mixture of the **PABA-OH**$^+$ and **PABA-NH$_3$**$^+$ protomers.

Whilst Fig. 2b clearly shows that two protomers of PABA·H^+ are present in the gas phase, the overlap between bands **II** and **III** means that both the **PABA-OH**$^+$ and **PABA-NH$_3$**$^+$ isomers are present and cannot be resolved in this spectrum. Photodepletion measures the total absorbance of an ion population and thus combines all of the distinctive photophysical

mechanisms that cause ions to fragment. However, it is possible to resolve these separate photoexcitation (and photodecay) channels through inspection of the various photofragmentation channels.[14, 29, 42] Therefore, in the next section, we turn to exploring the photofragmentation behaviour that accompanies excitation of bands **I-IV** in an attempt to resolve the protomeric contributions to each of the absorption bands.

Photofragmentation mass spectra of PABA·H$^+$

Fig. 3a shows the photofragment mass spectrum of PABA·H$^+$ electrosprayed from an aqueous solution, photoexcited at the absorption maximum of 3.63 eV (peak of band **I**). As discussed above, the structure of the PABA·H$^+$ ion produced under these conditions should be solely **PABA-OH$^+$**. The most prominent fragments in the photofragment mass spectrum (Fig. 3a) are the m/z 120 and 94 fragments. These fragments have been observed as the primary fragments in previous CID and IRMPD experiments, where they were attributed respectively to the loss of water and carbon dioxide from **PABA-OH$^+$**.[2, 11] The production of fragments associated with loss of water and carbon dioxide is entirely consistent with the presence of a protonated carboxylic acid group. Detailed fragmentation mechanisms and production enthalpies of these fragments from the **PABA-OH$^+$** isomer were calculated by Kass.[11] Other prominent photofragments are observed with m/z 65, 77, 92, 93 and 95.

The photofragment mass spectrum of PABA·H^+ produced from an electrosprayed solution of MeCN and irradiated at 4.56 eV is given in Fig. 3b. This spectrum contains all of the photofragments observed in Fig. 3a, albeit in different ratios, as well as additional prominent fragments with m/z 121 and 139. The m/z 121 fragment is important as it is associated with the loss of NH_3, and was observed in the previous CID experiments of Kass and co-workers.[2] The fragment with m/z 139 represents the loss of NH_3 followed by the addition of water, which is present within the ion trap, to produce protonated hydroxybenzoic acid. The observation of a fragment associated with loss of NH_3 is strong evidence for the presence of a PABA·H^+ protomer that contains a protonated NH_2 group. For reference, the photofragment mass spectrum of PABA·H^+ electrosprayed from the MeCN solution irradiated at 5.6 eV is given in Fig. S9 of the ESI†. This spectrum shows that as the photon energy increases,

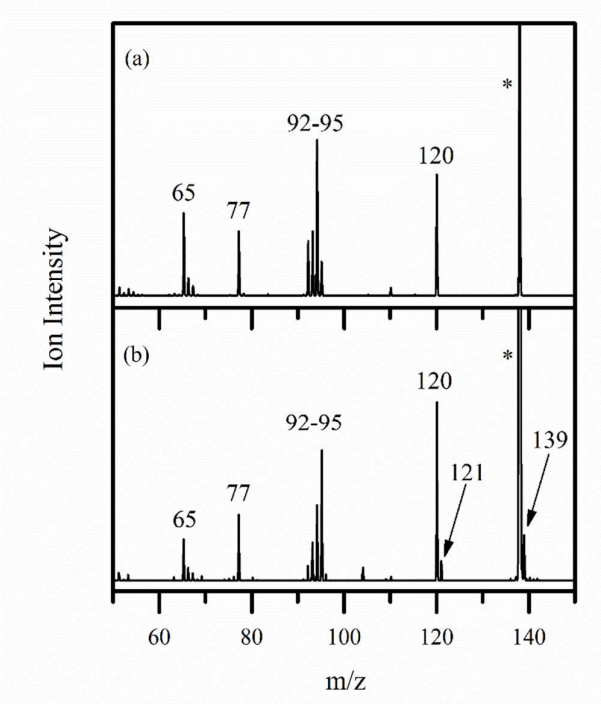

Fig. 3 Photofragment mass spectra of PABA·H^+, a) electrosprayed from an aqueous solution of PABA and excited at 3.63 eV; b) electrosprayed from a solution of PABA in MeCN and excited at 4.56 eV. * indicates the PABA·H^+ ion signal.

PABA-NH_3^+ fragmentation becomes more extensive and favours the production of m/z 65. A fragment with m/z 65, assigned as $C_5H_5^+$, was observed as a prominent fragment in a previous IRMPD study of the PABA radical cation and the *para*-amino benzoyl cation.[43] An additional prominent fragmentation route of **PABA-NH_3^+** at high photon energies is the loss of a hydrogen radical (m/z 137).

Photofragment production spectra of PABA·H^+ fragments

Having discussed the identities of the PABA·H^+ photofragments, we now turn to exploring the production spectra for the primary photofragments. These spectra are useful as they allow different decay pathways that contribute to the overall photodepletion spectrum to be resolved. For the case where two protomeric species contribute to the overall photodepletion spectrum, inspection of the photofragment action spectra may provide a route for assigning different protomer contributions.

Fig. 4a shows the production spectrum of the m/z 93 photofragment which is produced from PABA·H^+ electrosprayed from water. The shape of the spectrum displayed in Fig. 4a strongly resembles the photodepletion spectrum shown in Fig. 2a. This observation is unsurprising as the water-electrosprayed PABA·H^+ ion is expected to correspond solely to **PABA-OH^+**. Bands **I** and **II** appear to display some finer structure that is unresolved for the ambient temperature ions studied here. (Section S5 of the ESI† presents a deconvolution of the observed bands).

The photofragment production spectrum also displays two additional weak bands, centred at 4.47 and 5.72 eV, which are indistinguishable from experimental noise in the photodepletion spectrum (Fig. 4a).

Fig. 4b presents the summed photofragment production spectra for all of the prominent photofragments that are only observed when PABA is electrosprayed from a MeCN solution, namely m/z 121, 137 and 139 (see Fig. 3b and Section S3 of the ESI†). These fragments are primarily associated with the **PABA-NH$_3^+$** protomer and therefore resolve the UV spectrum of **PABA-NH$_3^+$** with only a minor contamination from **PABA-OH$^+$**. Bands **III** and **IV** again display partially resolved sub-structure (a deconvolution of these bands is also presented in Section S5 of the ESI†). Band **IV** is notably weaker in Fig. 4b when compared to the photodepletion spectrum recorded when electrospraying PABA from MeCN (Fig. 2b). This can be explained as arising from secondary fragmentation of the primary photofragments between 5.6 – 5.8 eV. Over this spectral range the photofragments with m/z 121 and 139

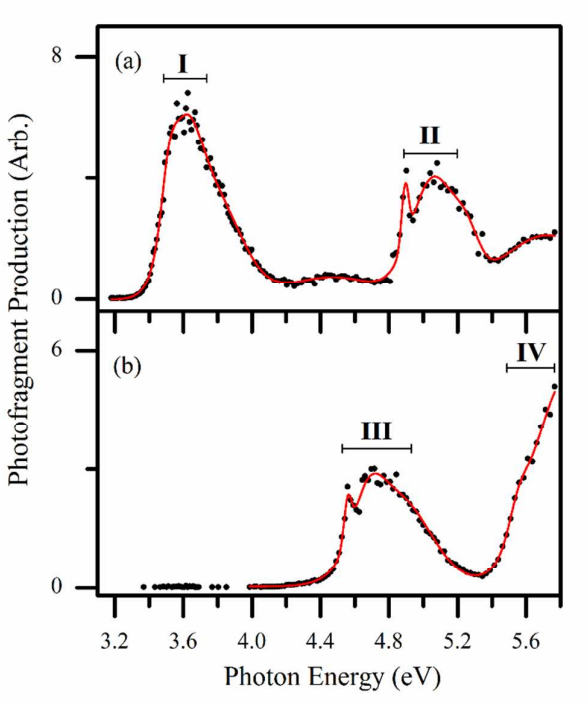

Fig. 4 Photofragment production spectra of the photofragments with a) m/z 93, from PABA·H$^+$ electrosprayed from water; b) the sum of the fragments with m/z 121, 137 and 139, from PABA·H$^+$ electrosprayed from MeCN. Fragments are produced following photoexcitation of mass-selected PABA·H$^+$ ions, across the range 3.2-5.8 eV.

reduce in intensity, but this reduction is associated with a concomitant increase in the fragment with m/z 65, namely $C_5H_5^+$. (Fig. S3 of the ESI†).

The structure of protonated PABA in aqueous solution was first investigated in 1943 using solution-phase UV absorption spectroscopy, and assigned as **PABA-NH$_3^+$**.[28] Following our assignment of the spectrum shown in Fig. 4b as arising solely from a **PABA-NH$_3^+$** protomer, we therefore expect that this spectrum should resemble the aqueous acidic UV-VIS absorption spectrum. For ease of comparison, the solution phase UV absorption spectra of PABA in both water and MeCN have been recorded as part of this study, and are included in the ESI† (Section S3). In both mildly acidic water and MeCN, the absorption onset occurs above 3.8 eV, with three main bands with $\lambda_{max,}$ of ~4.5, 4.6 and 5.5 eV, strikingly like the spectrum shown in Fig. 4b which is attributed to **PABA-NH$_3^+$**. Indeed, the absence of absorption in the solution-phase spectrum below 3.8 eV suggests that the **PABA-OH$^+$** protomer (Gaseous λ_{max} ~ 3.6 eV), is completely absent from the solution phase when the solvent is water or MeCN.

Calculated excitation spectra of PABA-OH$^+$ and PABA-NH$_3^+$

Electronic absorption spectra of the **PABA-OH$^+$** and **PABA-NH$_3^+$** protomers were calculated to determine the nature of the experimental electronic transitions and to test the spectral assignments. Initially, structures of PABA protonated at every carbon, nitrogen and oxygen gave were calculated using Gaussian 09. The structures were optimised as isolated ions as well as solvated ions with a water or acetonitrile solvent implicitly described using the polarisation continuum model (PCM). Table 1 lists the relative energies of the **PABA-OH$^+$** and **PABA-NH$_3^+$** structures in each local environment. (A complete list of calculated stable gaseous structures and structural energies is given in the ESI†). Table 1 shows that in the gas

phase, protonation at the carboxylic acid group is more stable than protonation at the amine by 33.7 kJ mol^{-1}. Upon solvation (in either water or acetonitrile), the relative energies of these structures swap to favour protonation at the amine, the carboxylic acid protonated structure is less stable by 32.9 and 31.4 kJ mol^{-1} in water and MeCN respectively. These calculations are in good agreement with the previously calculated proton affinities.[2, 11]

The excitation spectra of the two observed protomers of PABA have been calculated using the MRCI and SORCI methods, implemented by the quantum chemistry package ORCA. Table 2 lists the calculated and experimental vertical transition energies and transition intensities across the experimental spectral range. The experimental vertical transition energies of **PABA-OH$^+$** and **PABA-NH$_3^+$** were taken from the lowest-energy deconvoluted band components of bands of the Fig. 4a spectrum.

Table 2 shows that both the SORCI and MRCI computational methods can accurately predict the vertical transitions observed in the experimental spectrum. With **PABA-OH$^+$**, both methods predict excitation to the first excited state (band **I**) to be the most intense transition, with excitations around ~4.9 eV being considerably weaker. Notably, both calculation methods predict the existence of two weak bands around 4.4 and 5.7 eV, and although these bands are not well resolved in the experimental photodepletion spectrum, they are clearly present in the photofragment production spectrum of the m/z 93 photofragment (Fig 4a). This confirms that the photofragment-resolved peaks are caused by weak electronic transitions and are not artefacts relating to experimental error or multi-photon effects. For **PABA-NH$_3^+$**, the computational transitions confirm that this protomer is not associated with any UV absorption below ~4.5 eV. Both methods additionally show that the absorption cross section of band **III** is significantly weaker than band **IV**, reproducing the trends observed in

Table 1 Relative computed energies of the optimised **PABA-OH**$^+$ and **PABA-NH$_3$**$^+$ protomers. Structures were optimised as isolated gaseous ions or as solvated ions, using the PCM method to implicitly describe solvation by water or acetonitrile (MeCN). Energies were calculated using the B3LYP functional with the 6-311+G(2d,2p) basis set.

Solvation Scheme	Relative Electronic Energy / kJ mol^{-1}	
	PABA-OH$^+$	**PABA-NH$_3$**$^+$
Gaseous	0.0	33.7
Water	32.9	0.0
MeCN	31.4	0.0

the photodepletion spectrum (Fig. 2b). The calculated oscillator strengths suggest that **PABA-OH**$^+$ is spectrally brighter than **PABA-NH$_3$**$^+$ across the experimental range, with the MRCI calculations predicting band **I** to be more than twice as bright as band **IV.** This trend is indeed observed in the photodepletion spectra, with the maximum absorption of the **PABA-OH**$^+$ protomer occurring with approximately three times the maximum absorption of the **PABA-NH$_3$**$^+$ protomer. When comparing the two computational methods, the MRCI method is more accurate, with a mean absolute error (MAE) across the six transitions of 0.07 eV compared with 0.17 eV for SORCI excitations. The reference-space molecular orbitals that were used in the MRCI and SORCI excited state calculations are given in Section S2 of the ESI† along with a tabulated list of the orbital transitions that contribute to each excitation. We note that the nature of all of the experimental excitations are $\pi \rightarrow \pi^*$.

TDDFT excitation spectra were calculated for both protomers of PABA·H$^+$, and these results are also presented in Section S2 of the ESI†. TDDFT correctly predicts that the onset of

Table 2 Experimental and calculated vertical excitation energies (in eV) of the **PABA-OH**$^+$ and **PABA-NH$_3$**$^+$ structures of PABA·H$^+$ with the associated oscillator strengths (osc.) given in brackets. Excitation energies are predicted using the multi-reference configuration interaction (MRCI) and spectroscopy oriented CI (SORCI) methods. *

Excitation	**PABA-OH**$^+$			**PABA-NH$_3$**$^+$		
	Exp.	SORCI (osc.)	MRCI (osc.)	Exp.	SORCI (osc.)	MRCI (osc.)
$S_1 \leftarrow S_0$	3.51	3.73 (0.675)	3.58 (0.625)	4.56	4.72 (0.008)	4.50 (0.070)
$S_2 \leftarrow S_0$	4.47	4.45 (0.005)	4.26 (0.000)	5.56	5.84 (0.061)	5.60 (0.279)
$S_3 \leftarrow S_0$	4.89	5.09 (0.148)	4.89 (0.164)	-	6.68 (0.811)	6.23 (0.511)
$S_4 \leftarrow S_0$	5.72	5.87 (0.018)	5.71 (0.003)	-	6.75 (0.578)	6.30 (0.681)

* Details of the calculations are given in Section S2 of the ESI†.

electronic absorption of the **PABA-OH**$^+$ structure occurs at lower photon energies than the **PABA-NH$_3$**$^+$ structure. TDDFT also correctly predicts that the brightest transitions across the studied spectral range are $\pi \rightarrow \pi^*$ in nature. However, while the TDDFT calculations clearly reproduce the key trends of the experimental data, they struggle to accurately reproduce the experimentally observed transition energies.

Quantitative analysis of PABA·H$^+$ structure distributions

The above results sections have shown that electronic transitions within the **PABA-NH$_3$**$^+$ protomer only occur above 4.5 eV, any spectral feature below 4.5 eV must therefore be associated with the **PABA-OH**$^+$ protomer. As a result of this, the reduction in intensity of band **I** from the water-electrosprayed to MeCN-electrosprayed absorption spectra will be solely indicative of the reduction in abundance of the **PABA-OH**$^+$ protomer. By measuring

the reduction in photodepletion intensity at the 3.63 eV maximum in Fig. 2a and 2b (~42 and ~4 respectively), we estimate that the **PABA-OH**$^+$ to **PABA-NH$_3$**$^+$ ratio in the MeCN-electrosprayed spectrum is approximately 1:9. This indicates a significant reduction in population of the **PABA-OH**$^+$ protomer, which was assigned as the sole protomer in the water-electrosprayed spectrum.

Concluding Remarks

The results presented above demonstrate that UVPD spectroscopy within a laser-interfaced commercial mass spectrometer represents a suitable technique for distinguishing between the protomers of the PABA·H$^+$ system. These measurements were facilitated by the fact that when PABA is protonated at the amine or the carboxylic acid group, the electronic structures of the two resulting protomers are distinctive, and therefore their absorption spectral profiles are also very different. While the overall photodepletion spectrum of PABA·H$^+$ contains contributions from the two protomers, the spectral profiles of the individual protomers are clearly resolved when the photofragmentation production spectra of suitable photofragments (unique to a particular protomer) are inspected. The results we present above are entirely consistent with previous studies of electrosprayed PABA, where electrospray from aqueous solutions has been found to result purely in the **PABA-OH**$^+$ protomer, whereas a mixture of **PABA-OH**$^+$ and **PABA-NH$_3$**$^+$ protomers is produced when the solvent is acetonitrile.[2,11]

An additional key result to emerge from this work is that the protomer-resolved gas-phase ion spectroscopy demonstrated here provides a basis for identifying dominant protomeric species that are present in solution. Comparison of the protomer-resolved gas-phase absorption spectra, with the solution-phase UV spectra have revealed that the amine-protonated species is dominant in bulk solution. This result is in accord with past analysis of PABA solutions, and is certainly not a surprising result for this very well characterized system. However, it

does demonstrate that the methodology employed here has potential as an important diagnostic tool for identifying protomeric species present in solutions, i.e. the UV spectrum of a given protomer is essentially the same in the gas-phase and in the solution-phase (ignoring any solvent shift), thus allowing us to identify a species that is present in solution once the same isomer has been spectroscopically identified in the gas-phase.

Given the fact that there are now a growing number of fundamental studies that have clearly established that the protonation or deprotonation sites of electrosprayed ions are solvent-dependent,[1-4, 9-12] this factor frequently seems to be ignored when protomeric or deprotomeric molecular systems are investigated following electrospray preparation. The number of such studies has grown significantly over recent years,[15, 44] with a particular focus on biologically (or catalytically) relevant molecular systems. It would seem important that the effects of changing solvent on the spectroscopic or spectrometric results are explored, or better still, that the geometric structure of the protomer (or deprotomer) structure is definitively identified prior to further characterization. To date, in studies where this has been done it was either achieved using IR spectroscopy or via ion mobility mass spectrometry (IMMS).[4-13] Both approaches suffer from some limitations: For IR spectroscopy, free-electron lasers are often used to supply the IR photons, which introduces logistical and access restrictions. Alternatively, when bench top IR OPO/OPA laser systems are employed, there can be problems relating to insufficient absorption of photons in IRMPD to reach the dissociation threshold which can mean that certain protomeric systems are effectively spectroscopically dark.[11] For IMMS, the calculation of reliable collision cross sections for protomeric systems can be challenging.[5,7,9] The results presented in this work illustrate an alternative *in situ* approach for determining protonation sites in electrospray ions with suitable chromophores, using straightforward instrumentation.

Acknowledgements

We thank the University of York and the Department of Chemistry at the University of York for provision of funds for the Horizon OPO laser system, as well as the York Advanced Research Computing Cluster (YARCC) for access to computational resources.

Notes and References

1 Z. X. Tian and S. R. Kass, *J. Am. Chem. Soc.*, 2008, **130**, 10842-10843.

2 Z. X. Tian and S. R. Kass, *Angew. Chem. Int. Ed.*, 2009, **48**, 1321-1323.

3 Z. X. Tian, X. B. Wang, L. S. Wang and S. R. Kass, *J. Am. Chem. Soc.*, 2009, **131**, 1174-1181.

4 D. Schroder, M. Budesinsky and J. Roithova, *J. Am. Chem. Soc.*, 2012, **134**, 15897-15905.

5 J. Boschmans, S. Jacobs, J. P. Williams, M. Palmer, K. Richardson, K. Giles, C. Lapthorn, W. A. Herrebout, F. Lemiere and F. Sobott, *Analyst*, 2016, **141**, 4044-4054.

6 H. X. Xia and A. B. Attygalle, *Anal. Chem.*, 2016, **88**, 6035-6043.

7 R. S. Galaverna, G. A. Bataglion, G. Heerdt, G. F. de Sa, R. Daroda, V. S. Cunha, N. H. Morgon and M. N. Eberlin, *Eur. J. Org. Chem.*, 2015, 2189-2196.

8 P. M. Lalli, B. A. Iglesias, H. E. Toma, G. F. de Sa, R. J. Daroda, J. C. Silva, J. E. Szulejko, K. Araki and M. N. Eberlin, *J. Mass. Spectrom.*, 2012, **47**, 712-719.

9 S. Warnke, J. Seo, J. Boschmans, F. Sobott, J. H. Scrivens, C. Bleiholder, M. T. Bowers, S. Gewinner, W. Schollkopf, K. Pagel and G. von Helden, *J. Am. Chem. Soc.*, 2015, **137**, 4236-4242.

10 J. Seo, S. Warnke, S. Gewinner, W. Schollkopf, M. T. Bowers, K. Pagel and G. von Helden, *Phys. Chem. Chem. Phys.*, 2016, **18**, 25474-25482.

11 J. Schmidt, M. M. Meyer, I. Spector and S. R. Kass, *J. Phys. Chem. A*, 2011, **115**, 7625-7632.

12 J. D. Steill and J. Oomens, *J. Am. Chem. Soc.*, 2009, **131**, 13570-13571.

13 T. M. Chang, J. S. Prell, E. R. Warrick and E. R. Williams, *J. Am. Chem. Soc.*, 2012, **134**, 15805-15813.

14 E. Matthews and C. E. H. Dessent, *J. Phys. Chem. A*, 2016, **120**, 9209-9216.

15 C. Iacobucci, S. Reale and F. De Angelis, *Angew. Chem. Int. Ed.*, 2016, **55**, 2980-2993.

16 A. J. Ingram, C. L. Boeser and R. N. Zare, *Chem. Sci.*, 2016, **7**, 39-55.

17 D. Schroder, *Acc. Chem. Res.*, 2012, **45**, 1521-1532.

18 J. Roithova, *Chem. Soc. Rev.*, 2012, **41**, 547-559.

19 UV photodissociation spectroscopy has been used to identifying gas-phase isomers previously, but in these cases, different protomers were obtained from isomerically pure solutions as shown in Refs [20] - [22]. Protonated nucleobase tautomers have also been studied by UV action spectroscopy [23]-[25]. We note that other isomers have been spectroscopically identified by UV photodissociation. Ref [26] provides a recent example where UV action spectroscopy has been used to identify peptide isomers generated via electron transfer dissociation."

20 G. Feraud, N. Esteves-Lopez, C. Dedonder-Lardeux and C. Jouvet, *Phys. Chem. Chem. Phys.*, 2015, **17**, 25755-25760.

21 C. S. Hansen, S. J. Blanksby and A. J. Trevitt, *Phys. Chem. Chem. Phys.*, 2015, **17**, 25882-25890.

22 G. Feraud, L. Domenianni, E. Marceca, C. Dedonder-Lardeux and C. Jouvet, *J. Phys. Chem. A*, 2017, **121**, 2580-2587.

23 C. Marian, D. Nolting and R. Weinkauf, *Phys. Chem. Chem. Phys.*, 2005, **7**, 3306-3316.

24 S. Øvad Pedersen, K. Støchkel, C. Skinnerup Byskov, L. Munksgaard Baggesen, and S. Brøndsted Nielsen, *Phys. Chem. Chem. Phys.* 2013, **15**, 19748-19752.

25 M. Berdakin, G. Feraud, C. Dedonder-Lardeux, C. Jouvet and G. A. Pino, *Phys. Chem. Chem. Phys.* 2014, **16**, 10643-10650.

26 H. T. H. Nguyen, C.J. Shaffer, R. Pepin, F. Turecek, *J. Phys. Chem. Lett.*., 2015, **6**, 4722-4727.

27 J. L. Campbell, A. M. C. Yang, L. R. Melo and W. S. Hopkins, *J. Am. Soc. Mass Spectrom.*, 2016, **27**, 1277-1284.

28 W. D. Kumler and L. A. Strait, *J. Am. Chem. Soc.*, 1943, **65**, 2349-2354.

29 E. Matthews, A. Sen, N. Yoshikawa, E. Bergstrom and C. E. H. Dessent, *Phys. Chem. Chem. Phys.*, 2016, **18**, 15143-15152.

30 M. J. Frisch, G. W. Trucks, H. B. Schlegel, G. E. Scuseria, M. A. Robb, J. R. Cheeseman, G. Scalmani, V. Barone, B. Mennucci, G. A. Petersson, H. Nakatsuji, M. Caricato, X. Li, H. P. Hratchian, A. F. Izmaylov, J. Bloino, G. Zheng, J. L. Sonnenberg, M. Hada, M. Ehara, K. Toyota, R. Fukuda, J. Hasegawa, M. Ishida, T. Nakajima, Y. Honda, O. Kitao, H. Nakai, T. Vreven, J. A. Montgomery Jr., J. E. Peralta, F. Ogliaro, M. J. Bearpark, J. Heyd, E. N. Brothers, K. N. Kudin, V. N. Staroverov, R. Kobayashi, J. Normand, K. Raghavachari, A. P. Rendell, J. C. Burant, S. S. Iyengar, J. Tomasi, M. Cossi, N. Rega, N. J. Millam, M. Klene, J. E. Knox, J. B. Cross, V. Bakken, C. Adamo, J. Jaramillo, R. Gomperts, R. E. Stratmann, O. Yazyev, A. J. Austin, R. Cammi, C. Pomelli, J. W. Ochterski, R. L. Martin, K. Morokuma, V. G. Zakrzewski, G. A. Voth, P. Salvador, J. J. Dannenberg, S. Dapprich, A. D. Daniels, Ö. Farkas, J. B. Foresman, J. V. Ortiz, J. Cioslowski and D. J. Fox, *Gaussian 09,* Revision D.01; Gaussian, Inc., Wallingford, CT, 2009.

31 A. D. Becke, *J. Chem. Phys.*, 1993, **98**, 5648-5652.

32 A. D. Mclean and G. S. Chandler, *J. Chem. Phys.*, 1980, **72**, 5639-5648.

33 R. Krishnan, J. S. Binkley, R. Seeger and J. A. Pople, *J. Chem. Phys.*, 1980, **72**, 650-654.

34 T. Clark, J. Chandrasekhar, G. W. Spitznagel and P. V. Schleyer, *J. Comput. Chem.*, 1983, **4**, 294-301.

35 M. J. Frisch, J. A. Pople and J. S. Binkley, *J. Chem. Phys.*, 1984, **80**, 3265-3269.

36 M. Headgordon, J. A. Pople and M. J. Frisch, *Chem. Phys. Lett.*, 1988, **153**, 503-506.

37 F. Neese, *WIREs Comput Mol Sci*, 2012, **2**, 73-78.

38 F. Neese, *J. Chem. Phys.*, 2003, **119**, 9428-9443.

39 T. H. Dunning, *J. Chem. Phys.*, 1989, **90**, 1007-1023.

40 Y. G. He, C. Y. Wu and W. Kong, *J. Phys. Chem. A*, 2005, **109**, 2809-2815.

41 Y. G. He, C. Y. Wu and W. Kong, *J. Chem. Phys.*, 2004, **121**, 3533-3539.

42 A. Sen and C. E. H. Dessent, *J. Phys. Chem. Lett.*, 2014, **5**, 3281-3285.

43 J. Oomens, D. T. Moore, G. Meijer and G. von Helden, *Phys. Chem. Chem. Phys.*, 2004, **6**, 710-718.

44 F. Coelho and M. N. Eberlin, *Angew. Chem. Int. Ed.*, 2011, **50**, 5261-5263.

Experiment and theory confirm that UV laser photodissociation spectroscopy can distinguish protomers formed via electrospray

Edward Matthews and Caroline E. H. Dessent*

Department of Chemistry, University of York, Heslington, York, YO10 5DD, UK.

Abstract

The identification of protonation sites in electrosprayed molecules remains a challenge in contemporary physical science. We present the first demonstration that low-resolution, UV laser photodissociation spectroscopy can be applied *in situ* to identify the protomers of *para*-aminobenzoic acid (PABA) formed via electrospray from a single solution. Electronic absorption spectra are recorded via photodepletion and photofragmentation for PABA electrosprayed from solutions of water and acetonitrile. Using this approach, two protomers can be straightforwardly identified, with only the carboxylic acid protomer being produced on electrospray from water while the amine-protonated isomer dominates upon electrospray from acetonitrile. High-level SORCI and MRCI calculations are presented to provide insight into the origin of the distinctive electronic spectra displayed by the protomers. Our results are in excellent agreement with previous PABA studies conducted using established techniques, and demonstrate that UV photodissociation spectroscopy of electrosprayed ions has potential as a new diagnostic tool for identifying protomeric species.

* Corresponding Author: caroline.dessent@york.ac.uk

Introduction

The influence of electrospray ionisation on the structure and properties of gaseous ions has been the subject of much debate in recent years, particularly in relation to the influence of electrospray on the location of protonation and deprotonation sites in the ions formed.[1-14] These studies are driven by the importance of acid-base reactions throughout chemistry and biology, so that correctly identifying the structures of protonation and deprotonation isomers can be crucial to understanding reactive processes. Electrospray ionization has been successfully employed across analytical chemistry for many years, and is now being increasingly used to probe solution-phase reactions and reactive intermediates for both chemical and biochemical systems.[15-18] The influence of the electrospray process on the location of protonation and deprotonation sites is therefore of ongoing key chemical interest. Moreover, it is of critical importance to develop innovative experimental methods that can determine the structures of gaseous protomers *in situ* following electrospray ionisation.

Protomer formation in small organic molecules following electrospray has been investigated by a number of mass-spectrometry methods. The effect of varying the electrospray source conditions (e.g. the solvent used in electrospray) on protomeric ratios was explicitly investigated in a number of these studies.[4,6] The first such studies employed collision induced dissociation as a structural tool,[1-3] and both ion mobility mass spectrometry (IMMS),[4-10] and infrared multiphoton dissociation (IRMPD) were subsequently employed.[9-13] These studies have led to an emerging view that the electrospray conditions can strongly influence the ratios of protomers or deprotomers obtained following electrospray.[11,12] This conclusion is in distinct contrast with the more traditional view that molecular ion populations obtained via electrospray

reflect the solution-phase populations.[4,11,12] Ultimately, this situation means that it is essential to have effective methodologies available that can experimentally identify protomeric species formed in the gas-phase via electrospray.

In a recent study, we investigated the electronic spectroscopy of the protonated form of the vitamin nicotinamide, generated via electrospray. [14] Our UV photodissociation (UVPD) results were consistent with two different protomers of nicotinamide being formed upon electrospray. This result suggested that UVPD spectroscopy could have potential as a new diagnostic spectroscopic tool for identifying protomeric isomers formed from a single solution.[19-22] UVPD spectroscopy offers considerable potential as a technique for identifying different protomers as resonant UV absorption is likely to be highly sensitive to the electronic structure of the chromophore.

In this work, we aim to evaluate UVPD for identifying electrosprayed protomers by investigating the prototype molecule, *para*-aminobenzoic acid (PABA). PABA has been extensively studied in both the solution phase and gas phases as a paradigm molecule which possesses two protonation sites (Fig. 1), namely the carboxylic oxygen (**PABA-OH$^+$**) and the amine nitrogen, (**PABA-NH$_3^+$**). While the **PABA-OH$^+$** protomer is the most stable protomer in the gas-phase, this situation is reversed in the solution phase where **PABA-NH$_3^+$** is most stable. [2, 10, 11, 13, 27, 28]

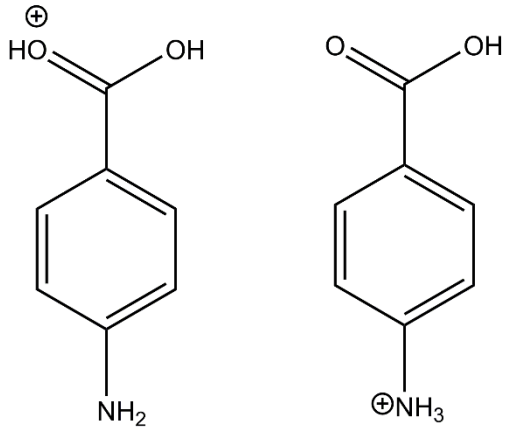

Fig. 1 Schematic diagram of the **PABA-OH⁺** and **PABA-NH₃⁺** protomers of PABA·H⁺, illustrating the lowest energy protonation sites.

From the previous studies of electrosprayed PABA, it has been established that the gaseous protomers produced depend strongly on the electrospray solvent. Kass and co-workers found that **PABA-OH⁺** was the only gaseous structure when a water/methanol solvent mixture was employed, while both the **PABA-NH₃⁺** and **PABA-OH⁺** protomers were observed when a water/acetonitrile solution was used.[2, 11] These results were subsequently confirmed in an IMMS and IRMPD study.[10] Williams and co-workers were able to demonstrate that the structure of microhydrated PABA·H⁺ moves from the **PABA-OH⁺** isomer to the **PABA-NH₃⁺** structure as the number of solvating water molecules increases.[13] Therefore, in this study, the UVPD spectra of protonated PABA produced from solutions of both water and acetonitrile will be measured, with the expectation that this change in solvent should produce dramatically different gaseous populations of the two possible protomers. This should allow us to firmly establish whether UVPD is able to distinguish such protomeric species, generated from a single solution. High-level SORCI and MRCI calculations are also performed to allow us to confirm

the spectroscopic assignments, as well as to provide a basis for understanding any differences in the electronic spectroscopy of different protomers.

Methodology

Experimental

The gaseous ion absorption spectra was recorded *in vacuo* using action spectroscopy. UV photodissociation experiments were conducted in an AmaZon ion-trap mass spectrometer, which was modified for the laser experiments as described in detail elsewhere.[14, 29] UV photons were produced by an Nd:YAG (10 Hz, Surelite) pumped OPO (Horizon) laser, giving ~1 mJ across the range 380 - 215 nm (3.26 – 5.77 eV). Scans were conducted using a 1 nm step size. Photofragmentation experiments were run with an ion accumulation time between 20 – 100 ms with a fragmentation time of 100 ms, ensuring an average of one laser pulse per ion packet. Total absorption is taken as the depletion in ion intensity of mass-selected PABA·H^+ ions, following irradiation, according to Equation [1]:

$$\text{Photodepletion Intensity} = \text{Ln}\left(\frac{\text{Int}_{\text{OFF}}}{\text{Int}_{\text{ON}}}\right)/\text{P}\lambda \qquad [1]$$

Where Int_{ON} and Int_{OFF} are the intensities of the PABA·H^+ ion signal with and without irradiation respectively, P is the tuneable laser power (mJ), and λ the wavelength (nm), following Ref [14]. (Section S1 of the ESI† presents power dependence measurements conducted as part of this work). The photodepletion intensities of mass selected PABA·H^+ ions have been averaged at each wavelength across the range 380 - 215 nm are plotted against the energy of the excitation photons. The production of photofragments that are associated with the depletion of PABA·H^+ ions is calculated using Equation [2], where Int_{Frag} is the ion intensity of an individual photofragment at a particular wavelength.

$$\text{Photofragmentation Production} = \left(\frac{\text{Int}_{\text{Frag}}}{\text{Int}_{\text{OFF}}}\right) / \text{P}\lambda \qquad [2]$$

Solutions of PABA (1 x 10^{-4} mol L^{-1}) in deionised water or acidified acetonitrile (32 µL acetic acid in 100 mL of MeCN) were introduced to the mass spectrometer through electrospray ionisation (ESI) using a nebulising gas pressure of 10.0 psi, an injection rate of 300 µL/hr, a drying gas flow rate of 8.0 L min^{-1}, and capillary temperatures of 140 and 200°C for water and MeCN respectively. A small volume of acetic acid was added to the MeCN solvent, since this was found to significantly improve the intensity and stability of the electrosprayed PABA·H^+ ion signal. Increasing the capillary temperature for MeCN also improved the stability of the ion signal. PABA was purchased from Fisher Scientific Ltd and used without purification. The voltages applied to the ion optics were tuned to maximise the ion signal of PABA·H^+ (m/z 138) using the automated tuning capabilities of the trapControl (Bruker) software.

Computational

Structures of PABA·H^+, protonated at each carbon, nitrogen and oxygen atom, were optimised using the B3LYP/6-311+G(2d,2p) functional and basis set using Gaussian 09.[30-35] Frequency calculations were performed to ensure that all optimised structures correspond to true energy minima. Time-dependent density functional theory (TDDFT) calculations were performed on the optimised structures of **PABA-NH_3^+** and **PABA-OH^+**, at the B3LYP/6-311+G(2d,2p) level. The B3LYP optimised structures of **PABA-NH_3^+** and **PABA-OH^+** were re-optimised at the MP2/6-311+G(2d,2p) level,[36] and these optimised structures were used as starting points in excited state calculations using the quantum chemical package ORCA.[37] Vertical excitation energies were calculated using the SORCI and MRCI methods,[38] with full details of the calculations given in Section S2 of the ESI†. These calculations used a CASSCF(6,6) reference space. Details of the generation and selection of orbitals are also given in the ESI†. All excited state calculations using ORCA were performed using the aug-cc-pVDZ basis set.[39]

Results and Discussion

Photodepletion absorption spectra of PABA·H$^+$

The UV absorption spectrum of mass-selected PABA·H$^+$, electrosprayed from water, is shown in Fig. 2a. This spectrum has an absorption onset at 3.3 eV and contains two well-resolved features; a strong band (**I**), observed between 3.4-4.1 eV (peaks between 3.6-3.8 eV), and a weaker band (**II**) that appears between 4.8-5.4 eV. We note that the "peak" of band **I** appears truncated in the spectrum shown in Fig. 2a. Power studies conducted at 3.63 eV (Section S1 of the ESI†), show that photodepletion is effectively flat for laser pulse energies > 0.6 mJ, indicating that all PABA·H$^+$ ions that spatially overlap with the laser are fragmenting at this excitation energy. Under the experimental conditions (laser pulse energy ~ 1 mJ), the water-electrosprayed photodepletion spectrum is therefore saturated between 3.55-3.75 eV.

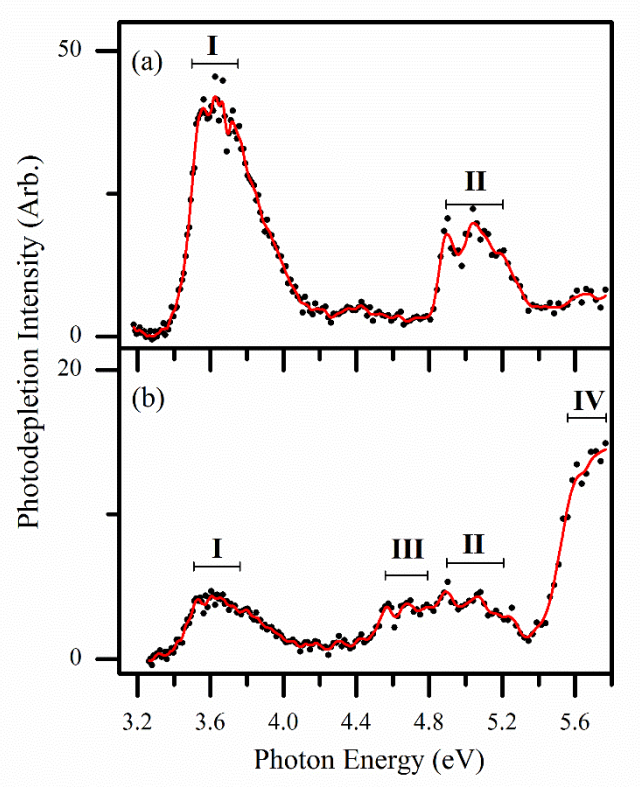

Fig. 2 UV absorption spectra of electrosprayed PABA·H$^+$ ions (m/z 138) across the range 3.26-5.77 eV (380-215 nm), produced from solutions of a) water and b) acidified-MeCN. The solid red lines are three-point adjacent averages of the data points.

Fig. 2b displays the corresponding UV absorption spectrum of PABA·H^+ formed from electrospray of a solution of acidified MeCN. The difference between this spectrum and the spectrum obtained from water is dramatic. The Fig. 2b spectrum contains the bands **I** and **II** that were observed in the spectrum of PABA·H^+ electrosprayed from water, along with two additional bands; a weak band between 4.5-4.8 eV (**III**) that overlaps with band **II**; and a strong band observed above 5.4 eV which peaks above 5.8 eV (**IV**). We note that fine structure can be seen in bands **II** and **III** of Fig. 2, and this is attributed to vibronic coupling which has been observed in the gaseous electronic absorption spectrum of neutral PABA.[40, 41] The observation of four absorption bands in the spectrum obtained from the MeCN solution, including the previously observed bands **I** and **II**, indicates that there are at least two distinctive species present in the gas phase when the PABA·H^+ ion is electrosprayed from MeCN. Since the irradiated ions have been mass-selected, the new species can be unambiguously assigned as a different structural isomer of PABA·H^+. The observation of one PABA·H^+ protomer when the electospray solvent is protic and two PABA·H^+ protomers when the solvent is aprotic is entirely expected from the previous studies reviewed in the introduction.[2, 11] Based on these previous studies, we therefore attribute the UV absorption spectrum obtained by electrospraying from an aqueous solution (Fig. 2a) as corresponding solely to the **PABA-OH$^+$** protomer, while the spectrum obtained by electrospraying from acetonitrile corresponds to a mixture of the **PABA-OH$^+$** and **PABA-NH$_3^+$** protomers.

Whilst Fig. 2b clearly shows that two protomers of PABA·H^+ are present in the gas phase, the overlap between bands **II** and **III** means that both the **PABA-OH$^+$** and **PABA-NH$_3^+$** isomers are present and cannot be resolved in this spectrum. Photodepletion measures the total absorbance of an ion population and thus combines all of the distinctive photophysical mechanisms that cause ions to fragment. However, it is possible to resolve these separate

photoexcitation (and photodecay) channels through inspection of the various photofragmentation channels.[14, 29, 42] Therefore, in the next section, we turn to exploring the photofragmentation behaviour that accompanies excitation of bands **I**-**IV** in an attempt to resolve the protomeric contributions to each of the absorption bands.

Photofragmentation mass spectra of PABA·H$^+$

Fig. 3a shows the photofragment mass spectrum of PABA·H$^+$ electrosprayed from an aqueous solution, photoexcited at the absorption maximum of 3.63 eV (peak of band **I**). As discussed above, the structure of the PABA·H$^+$ ion produced under these conditions should be solely **PABA-OH$^+$**. The most prominent fragments in the photofragment mass spectrum (Fig. 3a) are the m/z 120 and 94 fragments. These fragments have been observed as the primary fragments in previous CID and IRMPD experiments, where they were attributed respectively to the loss of water and carbon dioxide from **PABA-OH$^+$**.[2, 11] The production of fragments associated with loss of water and carbon dioxide is entirely consistent with the presence of a protonated carboxylic acid group. Detailed fragmentation mechanisms and production enthalpies of these fragments from the **PABA-OH$^+$** isomer were calculated by Kass.[11] Other prominent photofragments are observed with m/z 65, 77, 92, 93 and 95.

The photofragment mass spectrum of PABA·H^+ produced from an electrosprayed solution of MeCN and irradiated at 4.56 eV is given in Fig. 3b. This spectrum contains all of the photofragments observed in Fig. 3a, albeit in different ratios, as well as additional prominent fragments with m/z 121 and 139. The m/z 121 fragment is important as it is associated with the loss of NH_3, and was observed in the previous CID experiments of Kass and co-workers.[2] The fragment with m/z 139 represents the loss of NH_3 followed by the addition of water, which is present within the ion trap, to produce protonated hydroxybenzoic acid. The observation of a fragment associated with loss of NH_3 is strong evidence for the presence of a PABA·H^+ protomer that contains a protonated NH_2 group. For reference, the photofragment mass spectrum of PABA·H^+ electrosprayed from the MeCN solution irradiated at 5.6 eV is given in Fig. S9 of the ESI†. This spectrum shows that as the photon energy increases, **PABA-NH_3^+** fragmentation becomes more extensive and favours the production of m/z 65. A fragment with

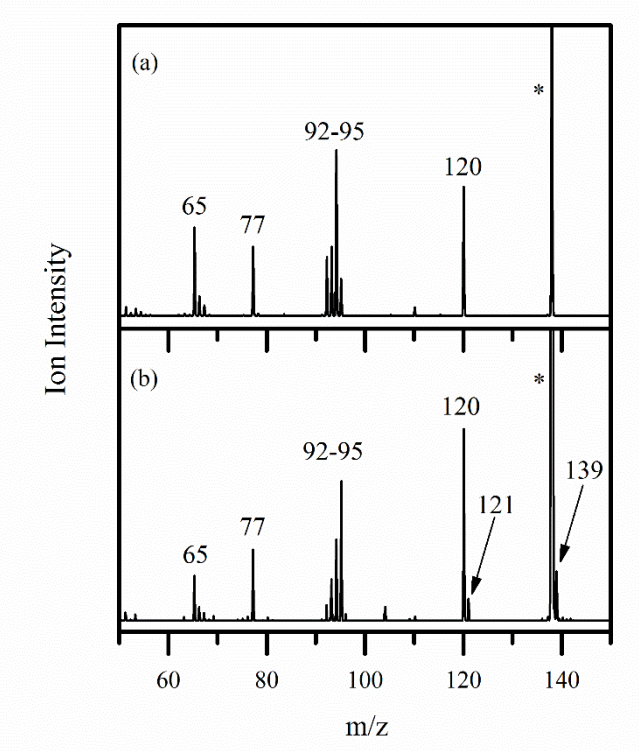

Fig. 3 Photofragment mass spectra of PABA·H^+, a) electrosprayed from an aqueous solution of PABA and excited at 3.63 eV; b) electrosprayed from a solution of PABA in MeCN and excited at 4.56 eV. * indicates the PABA·H^+ ion signal.

m/z 65, assigned as $C_5H_5^+$, was observed as a prominent fragment in a previous IRMPD study of the PABA radical cation and the *para*-amino benzoyl cation.[43] An additional prominent fragmentation route of **PABA-NH$_3$$^+$** at high photon energies is the loss of a hydrogen radical (m/z 137).

Photofragment production spectra of PABA·H$^+$ fragments

Having discussed the identities of the PABA·H$^+$ photofragments, we now turn to exploring the production spectra for the primary photofragments. These spectra are useful as they allow different decay pathways that contribute to the overall photodepletion spectrum to be resolved. For the case where two protomeric species contribute to the overall photodepletion spectrum, inspection of the photofragment action spectra may provide a route for assigning different protomer contributions.

Fig. 4a shows the production spectrum of the m/z 93 photofragment which is produced from PABA·H$^+$ electrosprayed from water. The shape of the spectrum displayed in Fig. 4a strongly resembles the photodepletion spectrum shown in Fig. 2a. This observation is unsurprising as the water-electrosprayed PABA·H$^+$ ion is expected to correspond solely to **PABA-OH$^+$**. Bands **I** and **II** appear to display some finer structure that is unresolved for the ambient temperature ions studied here. (Section S5 of the ESI† presents a deconvolution of the observed bands). The photofragment production spectrum also displays two additional weak bands, centred at 4.47 and 5.72 eV, which are indistinguishable from experimental noise in the photodepletion spectrum (Fig. 4a).

Fig. 4b presents the summed photofragment production spectra for all of the prominent photofragments that are only observed when PABA is electrosprayed from a MeCN solution, namely m/z 121, 137 and 139 (see Fig. 3b and Section S3 of the ESI†). These fragments are primarily associated with the **PABA-NH$_3$$^+$** protomer and therefore resolve the UV spectrum of **PABA-NH$_3$$^+$** with only a minor contamination from **PABA-OH$^+$**. Bands **III** and **IV** again display partially resolved sub-structure (a deconvolution of these bands is also presented in Section S5 of the ESI†). Band **IV** is notably weaker in Fig. 4b when compared to the photodepletion spectrum recorded when electrospraying PABA from MeCN (Fig. 2b). This can be explained as arising from secondary fragmentation of the primary photofragments between 5.6 – 5.8 eV. Over this spectral range the photofragments with m/z 121 and 139 reduce

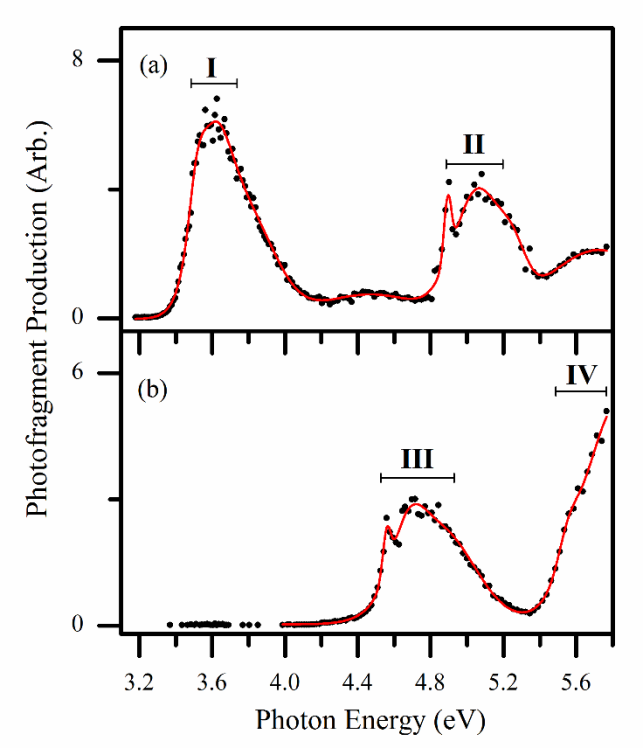

Fig. 4 Photofragment production spectra of the photofragments with a) m/z 93, from PABA·H$^+$ electrosprayed from water; b) the sum of the fragments with m/z 121, 137 and 139, from PABA·H$^+$ electrosprayed from MeCN. Fragments are produced following photoexcitation of mass-selected PABA·H$^+$ ions, across the range 3.2-5.8 eV.

in intensity, but this reduction is associated with a concomitant increase in the fragment with m/z 65, namely $C_5H_5^+$. (Fig. S3 of the ESI†).

The structure of protonated PABA in aqueous solution was first investigated in 1943 using solution-phase UV absorption spectroscopy, and assigned as **PABA-NH_3^+**.[28] Following our assignment of the spectrum shown in Fig. 4b as arising solely from a **PABA-NH_3^+** protomer, we therefore expect that this spectrum should resemble the aqueous acidic UV-VIS absorption spectrum. For ease of comparison, the solution phase UV absorption spectra of PABA in both water and MeCN have been recorded as part of this study, and are included in the ESI† (Section S3). In both mildly acidic water and MeCN, the absorption onset occurs above 3.8 eV, with three main bands with $\lambda_{max,}$ of ~4.5, 4.6 and 5.5 eV, strikingly like the spectrum shown in Fig. 4b which is attributed to **PABA-NH_3^+**. Indeed, the absence of absorption in the solution-phase spectrum below 3.8 eV suggests that the **PABA-OH^+** protomer (Gaseous λ_{max} ~ 3.6 eV), is completely absent from the solution phase when the solvent is water or MeCN.

Calculated excitation spectra of PABA-OH^+ and PABA-NH_3^+

Electronic absorption spectra of the **PABA-OH^+** and **PABA-NH_3^+** protomers were calculated to determine the nature of the experimental electronic transitions and to test the spectral assignments. Initially, structures of PABA protonated at every carbon, nitrogen and oxygen gave were calculated using Gaussian 09. The structures were optimised as isolated ions as well as solvated ions with a water or acetonitrile solvent implicitly described using the polarisation continuum model (PCM). Table 1 lists the relative energies of the **PABA-OH^+** and **PABA-NH_3^+** structures in each local environment. (A complete list of calculated stable gaseous structures and structural energies is given in the ESI†). Table 1 shows that in the gas phase, protonation at the carboxylic acid group is more stable than protonation at the amine by 33.7

kJ mol^{-1}. Upon solvation (in either water or acetonitrile), the relative energies of these structures swap to favour protonation at the amine, the carboxylic acid protonated structure is less stable by 32.9 and 31.4 kJ mol^{-1} in water and MeCN respectively. These calculations are in good agreement with the previously calculated proton affinities.[2, 11]

The excitation spectra of the two observed protomers of PABA have been calculated using the MRCI and SORCI methods, implemented by the quantum chemistry package ORCA. Table 2 lists the calculated and experimental vertical transition energies and transition intensities across the experimental spectral range. The experimental vertical transition energies of **PABA-OH$^+$** and **PABA-NH$_3^+$** were taken from the lowest-energy deconvoluted band components of bands of the Fig. 4a spectrum.

Table 2 shows that both the SORCI and MRCI computational methods can accurately predict the vertical transitions observed in the experimental spectrum. With **PABA-OH$^+$**, both methods predict excitation to the first excited state (band **I**) to be the most intense transition, with excitations around ~4.9 eV being considerably weaker. Notably, both calculation methods predict the existence of two weak bands around 4.4 and 5.7 eV, and although these bands are not well resolved in the experimental photodepletion spectrum, they are clearly present in the photofragment production spectrum of the m/z 93 photofragment (Fig 4a). This confirms that the photofragment-resolved peaks are caused by weak electronic transitions and are not artefacts relating to experimental error or multi-photon effects. For **PABA-NH$_3^+$**, the computational transitions confirm that this protomer is not associated with any UV absorption below ~4.5 eV. Both methods additionally show that the absorption cross section of band **III** is significantly weaker than band **IV**, reproducing the trends observed in the photodepletion spectrum (Fig. 2b). The calculated oscillator strengths suggest that **PABA-OH$^+$** is spectrally

Table 1 Relative computed energies of the optimised **PABA-OH$^+$** and **PABA-NH$_3^+$** protomers. Structures were optimised as isolated gaseous ions or as solvated ions, using the PCM method to implicitly describe solvation by water or acetonitrile (MeCN). Energies were calculated using the B3LYP functional with the 6-311+G(2d,2p) basis set.

Solvation Scheme	Relative Electronic Energy / kJ mol^{-1}	
	PABA-OH$^+$	**PABA-NH$_3^+$**
Gaseous	0.0	33.7
Water	32.9	0.0
MeCN	31.4	0.0

brighter than **PABA-NH$_3^+$** across the experimental range, with the MRCI calculations predicting band **I** to be more than twice as bright as band **IV.** This trend is indeed observed in the photodepletion spectra, with the maximum absorption of the **PABA-OH$^+$** protomer occurring with approximately three times the maximum absorption of the **PABA-NH$_3^+$** protomer. When comparing the two computational methods, the MRCI method is more accurate, with a mean absolute error (MAE) across the six transitions of 0.07 eV compared with 0.17 eV for SORCI excitations. The reference-space molecular orbitals that were used in the MRCI and SORCI excited state calculations are given in Section S2 of the ESI† along with a tabulated list of the orbital transitions that contribute to each excitation. We note that the nature of all of the experimental excitations are $\pi \rightarrow \pi^*$.

TDDFT excitation spectra were calculated for both protomers of PABA·H$^+$, and these results are also presented in Section S2 of the ESI†. TDDFT correctly predicts that the onset of electronic absorption of the **PABA-OH$^+$** structure occurs at lower photon energies than the

Table 2 Experimental and calculated vertical excitation energies (in eV) of the **PABA-OH$^+$** and **PABA-NH$_3^+$** structures of PABA·H$^+$ with the associated oscillator strengths (osc.) given in brackets. Excitation energies are predicted using the multi-reference configuration interaction (MRCI) and spectroscopy oriented CI (SORCI) methods. *

Excitation	**PABA-OH$^+$**			**PABA-NH$_3^+$**		
	Exp.	SORCI (osc.)	MRCI (osc.)	Exp.	SORCI (osc.)	MRCI (osc.)
$S_1 \leftarrow S_0$	3.51	3.73 (0.675)	3.58 (0.625)	4.56	4.72 (0.008)	4.50 (0.070)
$S_2 \leftarrow S_0$	4.47	4.45 (0.005)	4.26 (0.000)	5.56	5.84 (0.061)	5.60 (0.279)
$S_3 \leftarrow S_0$	4.89	5.09 (0.148)	4.89 (0.164)	-	6.68 (0.811)	6.23 (0.511)
$S_4 \leftarrow S_0$	5.72	5.87 (0.018)	5.71 (0.003)	-	6.75 (0.578)	6.30 (0.681)

* Details of the calculations are given in Section S2 of the ESI†.

PABA-NH$_3^+$ structure. TDDFT also correctly predicts that the brightest transitions across the studied spectral range are $\pi \rightarrow \pi^*$ in nature. However, while the TDDFT calculations clearly reproduce the key trends of the experimental data, they struggle to accurately reproduce the experimentally observed transition energies.

Quantitative analysis of PABA·H$^+$ structure distributions

The above results sections have shown that electronic transitions within the **PABA-NH$_3^+$** protomer only occur above 4.5 eV, any spectral feature below 4.5 eV must therefore be associated with the **PABA-OH$^+$** protomer. As a result of this, the reduction in intensity of band **I** from the water-electrosprayed to MeCN-electrosprayed absorption spectra will be solely indicative of the reduction in abundance of the **PABA-OH$^+$** protomer. By measuring the reduction in photodepletion intensity at the 3.63 eV maximum in Fig. 2a and 2b (~42 and ~4

respectively), we estimate that the **PABA-OH$^+$** to **PABA-NH$_3^+$** ratio in the MeCN-electrosprayed spectrum is approximately 1:9. This indicates a significant reduction in population of the **PABA-OH$^+$** protomer, which was assigned as the sole protomer in the water-electrosprayed spectrum.

Concluding Remarks

The results presented above demonstrate that UVPD spectroscopy within a laser-interfaced commercial mass spectrometer represents a suitable technique for distinguishing between the protomers of the PABA·H$^+$ system. These measurements were facilitated by the fact that when PABA is protonated at the amine or the carboxylic acid group, the electronic structures of the two resulting protomers are distinctive, and therefore their absorption spectral profiles are also very different. While the overall photodepletion spectrum of PABA·H$^+$ contains contributions from the two protomers, the spectral profiles of the individual protomers are clearly resolved when the photofragmentation production spectra of suitable photofragments (unique to a particular protomer) are inspected. The results we present above are entirely consistent with previous studies of electrosprayed PABA, where electrospray from aqueous solutions has been found to result purely in the **PABA-OH$^+$** protomer, whereas a mixture of **PABA-OH$^+$** and **PABA-NH$_3^+$** protomers is produced when the solvent is acetonitrile.[2,11]

An additional key result to emerge from this work is that the protomer-resolved gas-phase ion spectroscopy demonstrated here provides a basis for identifying dominant protomeric species that are present in solution. Comparison of the protomer-resolved gas-phase absorption spectra, with the solution-phase UV spectra have revealed that the amine-protonated species is dominant in bulk solution. This result is in accord with past analysis of PABA solutions, and is certainly not a surprising result for this very well characterized system. However, it does demonstrate that the methodology employed here has potential as an important diagnostic tool

for identifying protomeric species present in solutions, i.e. the UV spectrum of a given protomer is essentially the same in the gas-phase and in the solution-phase (ignoring any solvent shift), thus allowing us to identify a species that is present in solution once the same isomer has been spectroscopically identified in the gas-phase.

Given the fact that there are now a growing number of fundamental studies that have clearly established that the protonation or deprotonation sites of electrosprayed ions are solvent-dependent,[1-4, 9-12] this factor frequently seems to be ignored when protomeric or deprotomeric molecular systems are investigated following electrospray preparation. The number of such studies has grown significantly over recent years,[15, 44] with a particular focus on biologically (or catalytically) relevant molecular systems. It would seem important that the effects of changing solvent on the spectroscopic or spectrometric results are explored, or better still, that the geometric structure of the protomer (or deprotomer) structure is definitively identified prior to further characterization. To date, in studies where this has been done it was either achieved using IR spectroscopy or via ion mobility mass spectrometry (IMMS).[4-13] Both approaches suffer from some limitations: For IR spectroscopy, free-electron lasers are often used to supply the IR photons, which introduces logistical and access restrictions. Alternatively, when bench top IR OPO/OPA laser systems are employed, there can be problems relating to insufficient absorption of photons in IRMPD to reach the dissociation threshold which can mean that certain protomeric systems are effectively spectroscopically dark.[11] For IMMS, the calculation of reliable collision cross sections for protomeric systems can be challenging.[5,7,9] The results presented in this work illustrate an alternative *in situ* approach for determining protonation sites in electrospray ions with suitable chromophores, using straightforward instrumentation.

Acknowledgements

We thank the University of York and the Department of Chemistry at the University of York for provision of funds for the Horizon OPO laser system, as well as the York Advanced Research Computing Cluster (YARCC) for access to computational resources.

Notes and References

1 Z. X. Tian and S. R. Kass, *J. Am. Chem. Soc.*, 2008, **130**, 10842-10843.

2 Z. X. Tian and S. R. Kass, *Angew. Chem. Int. Ed.*, 2009, **48**, 1321-1323.

3 Z. X. Tian, X. B. Wang, L. S. Wang and S. R. Kass, *J. Am. Chem. Soc.*, 2009, **131**, 1174-1181.

4 D. Schroder, M. Budesinsky and J. Roithova, *J. Am. Chem. Soc.*, 2012, **134**, 15897-15905.

5 J. Boschmans, S. Jacobs, J. P. Williams, M. Palmer, K. Richardson, K. Giles, C. Lapthorn, W. A. Herrebout, F. Lemiere and F. Sobott, *Analyst*, 2016, **141**, 4044-4054.

6 H. X. Xia and A. B. Attygalle, *Anal. Chem.*, 2016, **88**, 6035-6043.

7 R. S. Galaverna, G. A. Bataglion, G. Heerdt, G. F. de Sa, R. Daroda, V. S. Cunha, N. H. Morgon and M. N. Eberlin, *Eur. J. Org. Chem.*, 2015, 2189-2196.

8 P. M. Lalli, B. A. Iglesias, H. E. Toma, G. F. de Sa, R. J. Daroda, J. C. Silva, J. E. Szulejko, K. Araki and M. N. Eberlin, *J. Mass. Spectrom.*, 2012, **47**, 712-719.

9 S. Warnke, J. Seo, J. Boschmans, F. Sobott, J. H. Scrivens, C. Bleiholder, M. T. Bowers, S. Gewinner, W. Schollkopf, K. Pagel and G. von Helden, *J. Am. Chem. Soc.*, 2015, **137**, 4236-4242.

10 J. Seo, S. Warnke, S. Gewinner, W. Schollkopf, M. T. Bowers, K. Pagel and G. von Helden, *Phys. Chem. Chem. Phys.*, 2016, **18**, 25474-25482.

11 J. Schmidt, M. M. Meyer, I. Spector and S. R. Kass, *J. Phys. Chem. A*, 2011, **115**, 7625-7632.

12 J. D. Steill and J. Oomens, *J. Am. Chem. Soc.*, 2009, **131**, 13570-13571.

13 T. M. Chang, J. S. Prell, E. R. Warrick and E. R. Williams, *J. Am. Chem. Soc.*, 2012, **134**, 15805-15813.

14 E. Matthews and C. E. H. Dessent, *J. Phys. Chem. A*, 2016, **120**, 9209-9216.

15 C. Iacobucci, S. Reale and F. De Angelis, *Angew. Chem. Int. Ed.*, 2016, **55**, 2980-2993.

16 A. J. Ingram, C. L. Boeser and R. N. Zare, *Chem. Sci.*, 2016, **7**, 39-55.

17 D. Schroder, *Acc. Chem. Res.*, 2012, **45**, 1521-1532.

18 J. Roithova, *Chem. Soc. Rev.*, 2012, **41**, 547-559.

19 UV photodissociation spectroscopy has been used to identifying gas-phase isomers previously, but in these cases, different protomers were obtained from isomerically pure solutions as shown in Refs [20] - [22]. Protonated nucleobase tautomers have also been studied by UV action spectroscopy [23]-[25]. We note that other isomers have been spectroscopically identified by UV photodissociation. Ref [26] provides a recent example where UV action spectroscopy has been used to identify peptide isomers generated via electron transfer dissociation."

20 G. Feraud, N. Esteves-Lopez, C. Dedonder-Lardeux and C. Jouvet, *Phys. Chem. Chem. Phys.*, 2015, **17**, 25755-25760.

21 C. S. Hansen, S. J. Blanksby and A. J. Trevitt, *Phys. Chem. Chem. Phys.*, 2015, **17**, 25882-25890.

22 G. Feraud, L. Domenianni, E. Marceca, C. Dedonder-Lardeux and C. Jouvet, *J. Phys. Chem. A*, 2017, **121**, 2580-2587.

23 C. Marian, D. Nolting and R. Weinkauf, *Phys. Chem. Chem. Phys.*, 2005, **7**, 3306-3316.

24 S. Øvad Pedersen, K. Støchkel, C. Skinnerup Byskov, L. Munksgaard Baggesen, and S. Brøndsted Nielsen, *Phys. Chem. Chem. Phys.* 2013, **15**, 19748-19752.

25 M. Berdakin, G. Feraud, C. Dedonder-Lardeux, C. Jouvet and G. A. Pino, *Phys. Chem. Chem. Phys.* 2014, **16**, 10643-10650.

26 H. T. H. Nguyen, C.J. Shaffer, R. Pepin, F. Turecek, *J. Phys. Chem. Lett.*., 2015, **6**, 4722-4727.

27 J. L. Campbell, A. M. C. Yang, L. R. Melo and W. S. Hopkins, *J. Am. Soc. Mass Spectrom.*, 2016, **27**, 1277-1284.

28 W. D. Kumler and L. A. Strait, *J. Am. Chem. Soc.*, 1943, **65**, 2349-2354.

29 E. Matthews, A. Sen, N. Yoshikawa, E. Bergstrom and C. E. H. Dessent, *Phys. Chem. Chem. Phys.*, 2016, **18**, 15143-15152.

30 M. J. Frisch, G. W. Trucks, H. B. Schlegel, G. E. Scuseria, M. A. Robb, J. R. Cheeseman, G. Scalmani, V. Barone, B. Mennucci, G. A. Petersson, H. Nakatsuji, M.

Caricato, X. Li, H. P. Hratchian, A. F. Izmaylov, J. Bloino, G. Zheng, J. L. Sonnenberg, M. Hada, M. Ehara, K. Toyota, R. Fukuda, J. Hasegawa, M. Ishida, T. Nakajima, Y. Honda, O. Kitao, H. Nakai, T. Vreven, J. A. Montgomery Jr., J. E. Peralta, F. Ogliaro, M. J. Bearpark, J. Heyd, E. N. Brothers, K. N. Kudin, V. N. Staroverov, R. Kobayashi, J. Normand, K. Raghavachari, A. P. Rendell, J. C. Burant, S. S. Iyengar, J. Tomasi, M. Cossi, N. Rega, N. J. Millam, M. Klene, J. E. Knox, J. B. Cross, V. Bakken, C. Adamo, J. Jaramillo, R. Gomperts, R. E. Stratmann, O. Yazyev, A. J. Austin, R. Cammi, C. Pomelli, J. W. Ochterski, R. L. Martin, K. Morokuma, V. G. Zakrzewski, G. A. Voth, P. Salvador, J. J. Dannenberg, S. Dapprich, A. D. Daniels, Ö. Farkas, J. B. Foresman, J. V. Ortiz, J. Cioslowski and D. J. Fox, *Gaussian 09,* Revision D.01; Gaussian, Inc., Wallingford, CT, 2009.

31 A. D. Becke, *J. Chem. Phys.*, 1993, **98**, 5648-5652.

32 A. D. Mclean and G. S. Chandler, *J. Chem. Phys.*, 1980, **72**, 5639-5648.

33 R. Krishnan, J. S. Binkley, R. Seeger and J. A. Pople, *J. Chem. Phys.*, 1980, **72**, 650-654.

34 T. Clark, J. Chandrasekhar, G. W. Spitznagel and P. V. Schleyer, *J. Comput. Chem.*, 1983, **4**, 294-301.

35 M. J. Frisch, J. A. Pople and J. S. Binkley, *J. Chem. Phys.*, 1984, **80**, 3265-3269.

36 M. Headgordon, J. A. Pople and M. J. Frisch, *Chem. Phys. Lett.*, 1988, **153**, 503-506.

37 F. Neese, *WIREs Comput Mol Sci*, 2012, **2**, 73-78.

38 F. Neese, *J. Chem. Phys.*, 2003, **119**, 9428-9443.

39 T. H. Dunning, *J. Chem. Phys.*, 1989, **90**, 1007-1023.

40 Y. G. He, C. Y. Wu and W. Kong, *J. Phys. Chem. A*, 2005, **109**, 2809-2815.

41 Y. G. He, C. Y. Wu and W. Kong, *J. Chem. Phys.*, 2004, **121**, 3533-3539.

42 A. Sen and C. E. H. Dessent, *J. Phys. Chem. Lett.*, 2014, **5**, 3281-3285.

43 J. Oomens, D. T. Moore, G. Meijer and G. von Helden, *Phys. Chem. Chem. Phys.*, 2004, **6**, 710-718.

44 F. Coelho and M. N. Eberlin, *Angew. Chem. Int. Ed.*, 2011, **50**, 5261-5263.

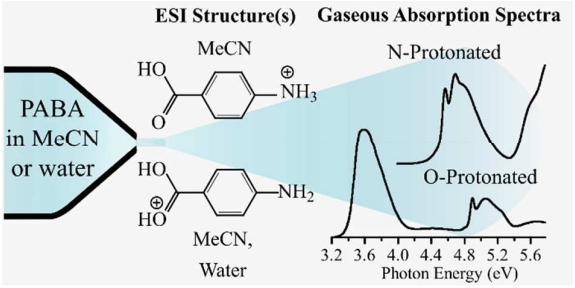

Low-resolution UV spectroscopy within a laser-interfaced commercial mass spectrometer can be used identify electrosprayed protomers of para-aminobenzoic acid (PABA).

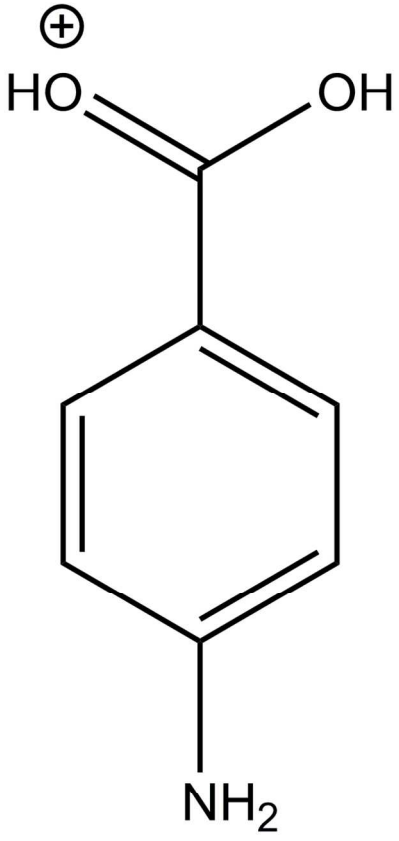

PABA-OH$^+$

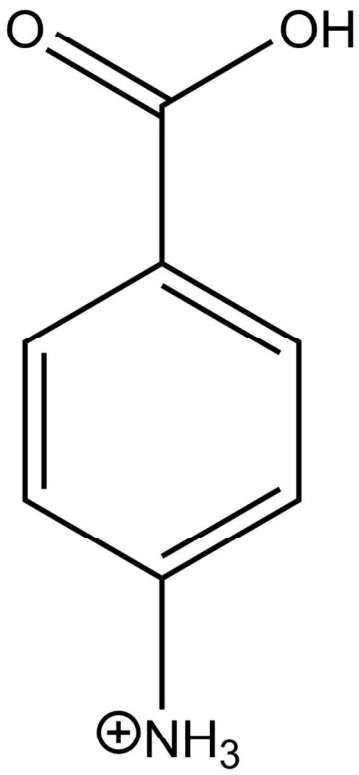

PABA-NH$_3^+$

419x419mm (96 x 96 DPI)

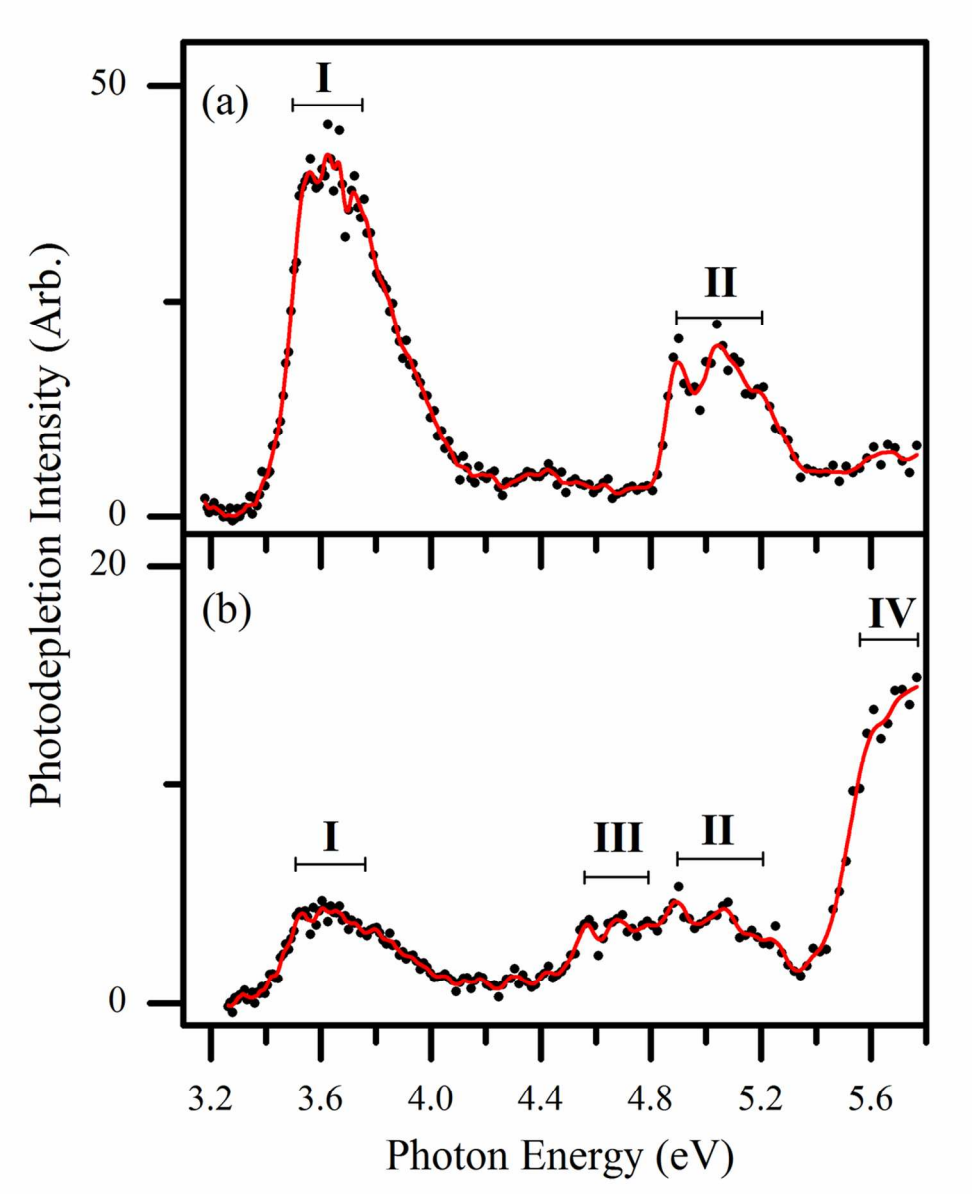

104x129mm (300 x 300 DPI)

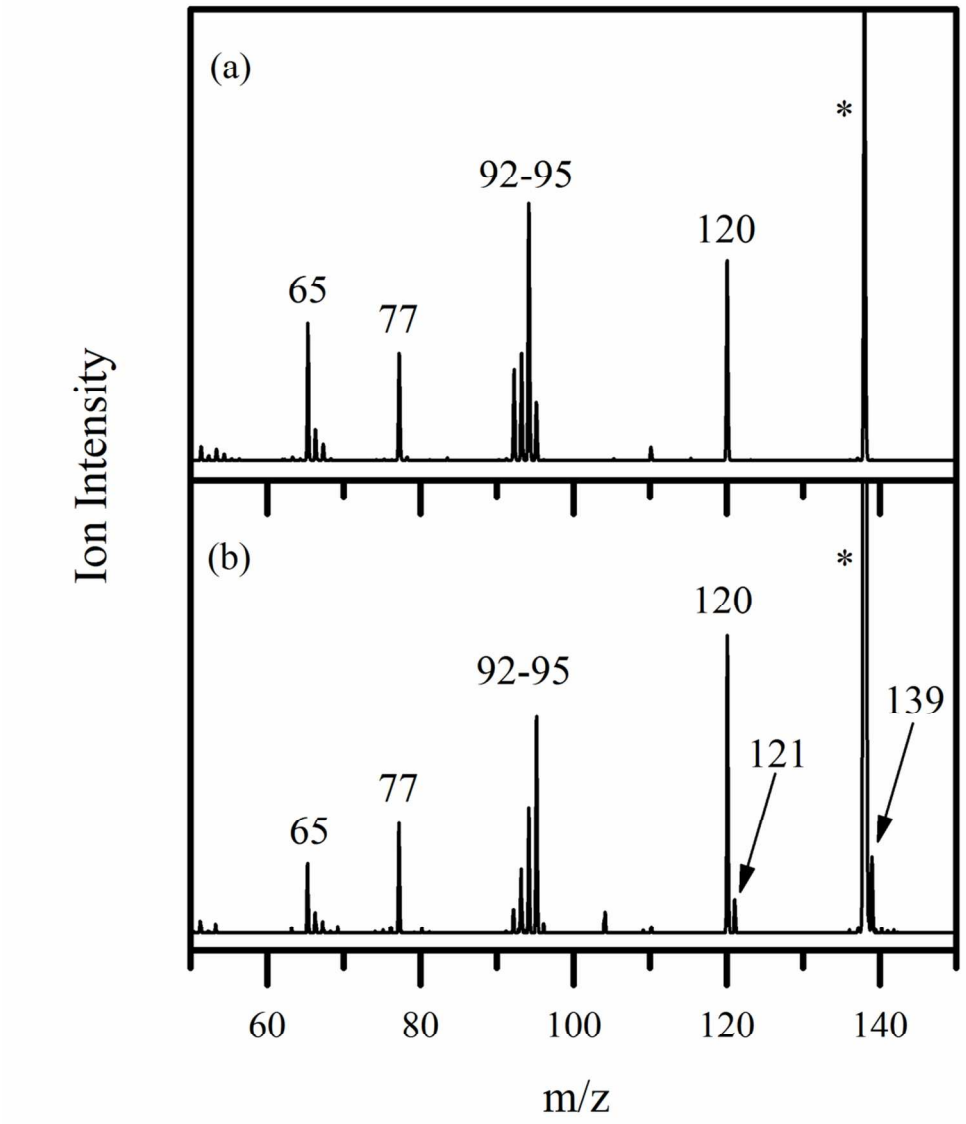

99x117mm (300 x 300 DPI)

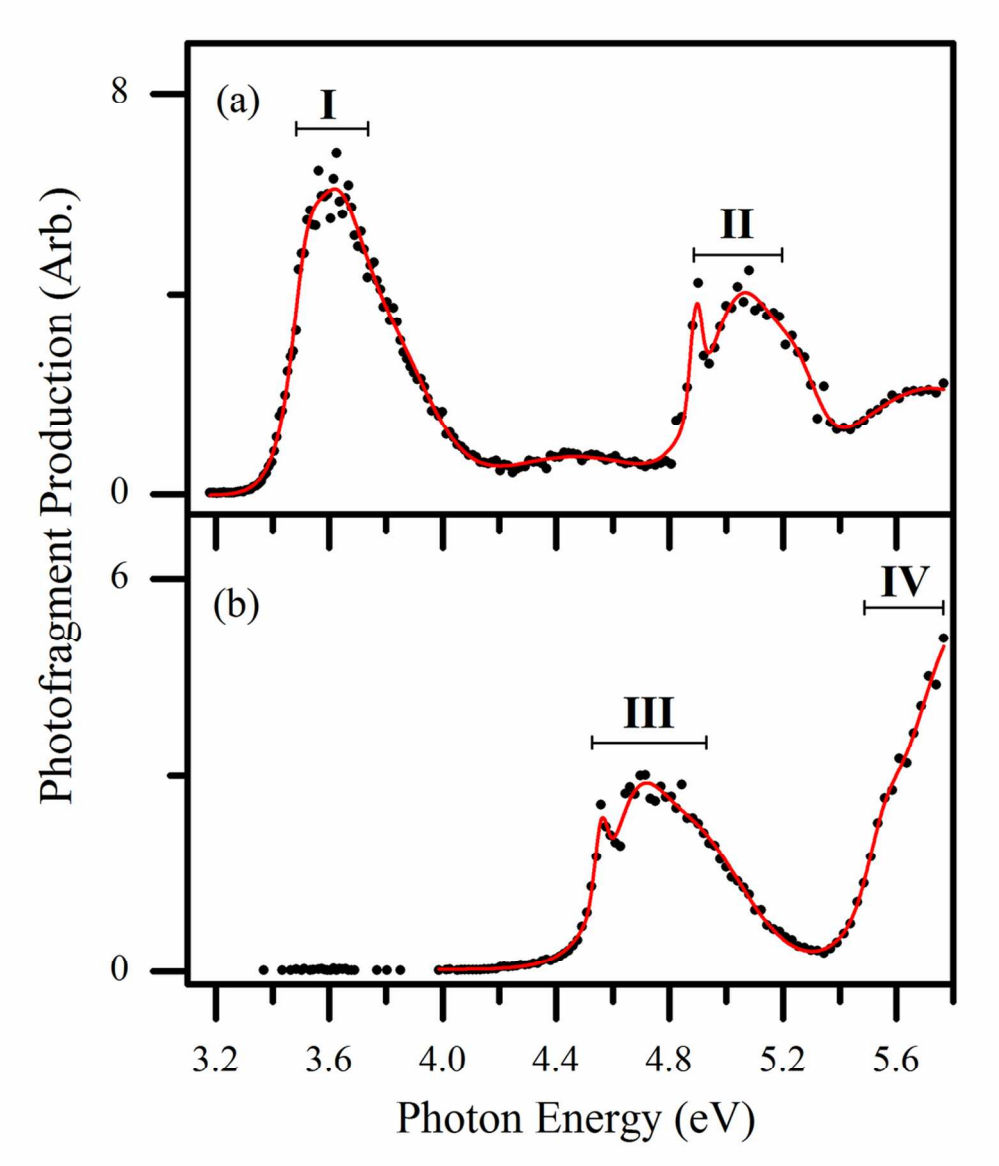

99x117mm (300 x 300 DPI)

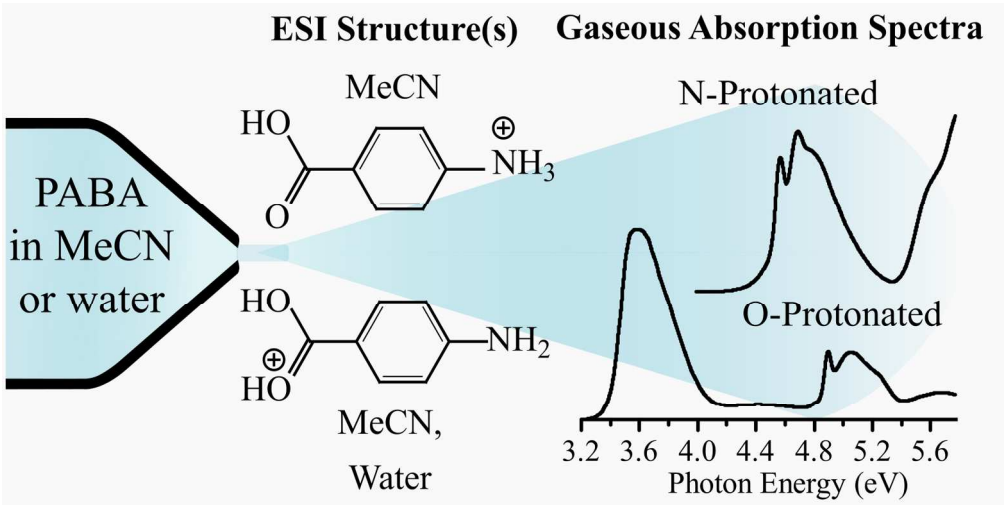

500x250mm (96 x 96 DPI)